Integrating Arctic plant functional types in a land surface model using above- and belowground field observations

Benjamin N. Sulman[1], Verity G. Salmon[1], Colleen M. Iversen[1], Amy Breen[2], Fengming Yuan[1] and Peter Thornton[1]

[1]Environmental Sciences Division and Climate Change Science Institute, Oak Ridge National Laboratory
[2]International Arctic Research Center, University of Alaska Fairbanks

*

Key points

- Biomass measurements of arctic plants in the Seward Peninsula were used to develop nine arctic plant functional types in the E3SM Land Model
- New plant functional types included mosses, lichens, graminoids, and shrubs of different height classes and leaf habits
- Simulations across a gradient of plant communities showed how variations in plant traits and soil depth drive different biomass patterns

Abstract

Accurate simulations of high latitude ecosystems are critical for confident Earth system model (ESM) projections of carbon cycle feedbacks to global climate change. Land surface model components of ESMs, including the E3SM Land Model (ELM), simulate vegetation growth and ecosystem responses to changing climate and atmospheric CO_2 concentrations by grouping heterogeneous vegetation into like sets of plant functional types (PFTs). Such models often represent high-latitude vegetation using only two PFTs (shrub and grass), thereby missing the diversity of vegetation growth forms and functional traits in the Arctic. Here, we use field observations of biomass and leaf traits across a gradient of plant communities on the Seward Peninsula in northwest Alaska to replace the original ELM configuration for the first time with

nine arctic-specific PFTs. The PFTs that are new to the model include: 1) nonvascular mosses and lichens, 2) deciduous and evergreen shrubs of various height classes, including an alder PFT, 3) graminoids, and 4) forbs. Improvements relative to the original model configuration included greater belowground biomass allocation, persistent fine roots and rhizomes of nonwoody plants, and better representation of variability in total plant biomass across sites with varying plant communities and depth to bedrock. Simulations through 2100 using the RCP8.5 climate scenario showed alder-dominated plant communities gaining more biomass and lichen-dominated communities gaining less biomass compared to default PFTs. Our results highlight how representing the diversity of arctic vegetation and confronting models with measurements from varied plant communities improves the representation of arctic vegetation in terrestrial ecosystem models.

Plain language summary:

Arctic ecosystems are home to specialized plant communities that have adapted to cold winters and short growing seasons. Arctic plant communities include a diverse group of plants with different heights and growth patterns, and these different types of plants are likely to respond differently to a warming climate and rising atmospheric carbon dioxide concentrations. However, the computer models that are used to predict how ecosystems and climate will change in the future include only a small number of Arctic plants. We used measurements of plant biomass across different plant communities in the Seward Peninsula of Alaska, USA to add new types of arctic plants to an ecosystem model. We then simulated how ecosystems would respond to a warming climate and rising levels of atmospheric carbon dioxide using both original and updated versions of arctic plants in the model. The new plant types allowed the model to simulate how ecosystems dominated by tall shrubs could gain biomass at much faster rates than ecosystems with thin soils and small plants. Our results show how including the diversity of arctic plants can improve model predictions of vegetation responses to climate change in the Arctic.

1 Introduction:

The Arctic region is warming twice as fast as the global average (Hartmann et al., 2013), driving substantial changes in both soil and vegetation dynamics in the region (Myers-Smith et al., 2019; Schuur et al., 2015; Turetsky et al., 2020). Earth system models, such as the Energy Exascale Earth System Model (E3SM; Golaz et al., 2019) rely on simulations of terrestrial ecosystems to provide the lower boundary conditions of the atmosphere and to simulate the terrestrial cycling of carbon (C), nutrients, water, and energy. Land surface models, including the E3SM Land Model (ELM) (Yang et al., 2019), simulate vegetation growth and mortality along with soil processes such as organic matter decomposition and hydrology. Permafrost soils in the Arctic hold an estimated 1300 Pg of organic C when integrated to 3-m depth (Hugelius et al., 2014). Thus, biogeochemical cycling in this region is critical to global climate simulations due to the potential for C cycle feedbacks to climate change, including increasing C emissions to the atmosphere due to decomposition of thawing permafrost (Koven et al., 2011; Schuur et al., 2015) or, conversely, increased arctic plant C uptake related to lengthening growing seasons, expanding shrub areas, or increasing nitrogen (N) availability (Myers-Smith et al., 2015; Qian et al., 2010; Salmon et al., 2016; Shaver et al., 1992).

Changes in the distribution of vegetation across the landscape, as well as in the composition and associated traits of tundra plant communities, also drive biophysical feedbacks to climate, including changes in albedo associated with shifting plant communities (Sturm et al., 2005) and changing transpiration rates associated with changes in leaf area and woody vegetation ranges (Pearson et al., 2013), as well as complex interactions among vegetation and soil temperature (Loranty et al., 2018). For example, vegetation height is a key factor in Arctic biophysical climate feedbacks. While trees and tall shrubs can extend above snow, decreasing winter albedo (Loranty et al., 2014) or driving earlier snowmelt (Wilcox et al., 2019), patches of taller vegetation can also trap snow, insulating the ground and keeping soils warmer during winter (Sturm et al., 2001). In turn, shading of the ground can exert a cooling effect during the warmer, snow-free season (Myers-Smith & Hik, 2013).

The Arctic is home to specialized low-stature tundra plant communities adapted to environmental and climatic extremes, with typically low summer temperatures and a short growing season. The region supports plants such as dwarf shrubs, forbs, lichens and mosses that all grow close to the ground. The amount of warmth available for plant growth increases as one moves south from the high Arctic, and the stature, abundance, and diversity of plants tends to increase as well. The distribution of plant communities is primarily controlled by landscape, topography, soil chemistry, soil moisture, and the plants that historically colonized an area (Raynolds et al., 2019; Thomas et al., 2020). In addition, plant communities also vary in their composition of plant functional types (PFTs), or groupings of plant species that share similar growth forms and roles in ecosystem function (Wullschleger et al., 2014).

In topographically and hydrologically diverse landscapes like the central Seward Peninsula of Alaska in the low Arctic, plant communities comprise a variety of graminoid, shrub, and lichen-dominated community types (Raynolds et al., 2019). In addition to canopy heights driving biophysical feedbacks, the varying growth patterns, biomass allocation patterns, and life history strategies of arctic PFTs result in an array of survival patterns and potential responses to warming (Bjorkman et al., 2018). Distributions of different arctic PFTs and traits are already changing under warming conditions (Epstein et al., 2012; Myers-Smith et al., 2011, 2015; Tape et al., 2006). As a result, accurate representation of the diversity of PFTs in arctic ecosystems, and of their specialized physiologies, is necessary to produce reliable model projections of arctic ecosystem responses to warming and other climatic changes (Rogers et al., 2017).

Arctic PFT classifications include evergreen and deciduous shrubs, forbs, graminoids (grasses, sedges, rushes), lichens, and bryophytes (mosses and liverworts) (Figure 2; Breen et al., 2020). These PFTs have been further differentiated by various factors such as by plant stature (dwarf, low, tall; Walker et al., 2005) or species (Sphagnum moss, Non-Sphagnum moss; Chapin et al. 1996). Key Arctic vegetation traits such as stature, leaf area, and leaf N are not well differentiated by the few and coarse functional groups typically used in land surface models (e.g., deciduous shrub, evergreen shrub, graminoid, and forb) (Thomas et al., 2019; Wullschleger et al., 2014). For example, a ubiquitous deciduous dwarf shrub such as *Salix arctica*, that is prostrate rather than erect, has a maximum height of a few centimeters and will not grow taller even under ideal environmental conditions. In contrast, low to tall erect shrubs may vary in height depending on habitat and growing season temperature. In one study, the deciduous low to tall shrub *Salix richardsonii* was shown to vary in maximum mean height across a latitudinal transect from approximately 10 cm in open tundra on the Alaskan arctic coast where mean July temperature was 2.6 ºC to >200 cm at streamside sites in the base of the foothills of the Brooks Range where mean July temperature was 10 ºC (D. A. Walker, 1987). Thus, changes in plant

biomass and height are constrained by the exact species or PFT present in a plant community. However, the current configuration of ELM, similar to other global land surface models such as the Community Land Model (CLM5; Lawrence et al., 2019), represents Arctic vegetation using only a small number of plant functional types (PFTs) (Wullschleger et al., 2014). In the default configuration of ELM used in global simulations (largely inherited from CLM4.5), arctic PFTs are divided into one broadleaf deciduous boreal shrub and one C3 arctic grass (Oleson et al., 2013). This structure limits the ability of the model to represent the diversity of growth forms in Arctic ecosystems as well as their associated responses to warming (Epstein et al., 2001). For example, the single boreal deciduous shrub PFT in ELM cannot represent the contrast in potential warming responses and biomass distributions of ecosystems dominated by shrub PFTs that differ in their stature and potential height. Because an increase in vegetation height in a dwarf-shrub dominated plant community often means a change in species composition (Bjorkman et al., 2018), a model lacking such trait variations among species might predict an inaccurate growth response to warming. Representation of vegetation trait variation has been shown to affect C cycling at global scales, making it a priority for improving the accuracy of ESMs (Verheijen et al., 2015).

In addition to missing variability in aboveground vegetation traits such as stature, models with few Arctic PFTs, such as ELM, also poorly represent above- and belowground partitioning of growth and biomass as observed in Arctic vegetation (Chapin et al., 1996; Song et al., 2017). In particular, Arctic shrubs and graminoids allocate a large fraction of their growth to belowground root and rhizome tissues that persist over multiple growing seasons (Iversen et al., 2015). A comparatively smaller fraction of growth is expressed in leaves and other aboveground tissues, which can persist for multiple seasons even in graminoids, reflecting the short growing season and resulting need for conservative growth strategies (Jonasson & Chapin, 1985; Shaver & Laundre, 1997). ELM, however, represents graminoids as deciduous plants that allow both leaves and fine roots to senesce every year. Graminoids in ELM only have leaf, fine-root, and nonstructural storage biomass pools, with no representation of rhizomes or other tissues that last more than a year, but which can be key to longevity and survival in environments with short growing seasons and cold winters (Van Groenendael et al., 1996) as well as providing the basis for lateral growth (Klimešová et al., 2018). Finally, ELM does not include specific representation of bryophyte or lichen growth or biomass. Many Arctic ecosystems are dominated by such cryptogam biomass (D. A. Walker et al., 2016), with important implications for carbon storage and responses to fire and grazing pressure (Joly et al., 2009; Longton, 1997). Bryophytes and lichens also have different albedo and other surface properties and do not transpire in the same way as vascular plants, making them important for accurately representing biophysical and hydrological interactions with the atmosphere in land surface models (Druel et al., 2019; Porada et al., 2016; Stoy et al., 2012).

As part of the Next Generation Ecosystem Experiment (NGEE) Arctic project, field sites were established on the Seward Peninsula of Alaska and plant composition, traits, and biomass allocation were characterized across hillslope and hydrological gradients, with the goal of evaluating and improving predictive capabilities of models in arctic ecosystems (Breen et al., 2020; Iversen et al., 2019b, 2019a; Salmon et al., 2019d, 2019c, 2019b data citations). For the purposes of this analysis, we used observations from six dominant plant communities spanning the Kougarok Hillslope field site located on the Seward Peninsula, AK (65°09'50.1"N, 164°49'34.2"W; see Figure 1) to parameterize Arctic-specific PFTs within ELM. We then used those PFTs in different assemblages and relative cover fractions to simulate the distinct plant

communities within ELM. We applied versions of ELM with configurations ranging from site-specific plant traits and community assemblies to a global-scale model grid cell to address two research questions: (1) *What is the relative importance of root-available soil depth, tundra plant species traits, and tundra plant community composition for improving model simulations of vegetation biomass and its variability across a landscape of low Arctic tundra plant communities?* (2) *How does the incorporation of measurement-constrained, tundra-specific plant functional types and soil depths affect projected vegetation biomass responses to increasing temperatures and atmospheric CO_2 concentrations over the 21st century?*

2 Methods:

2.1 Site and measurements

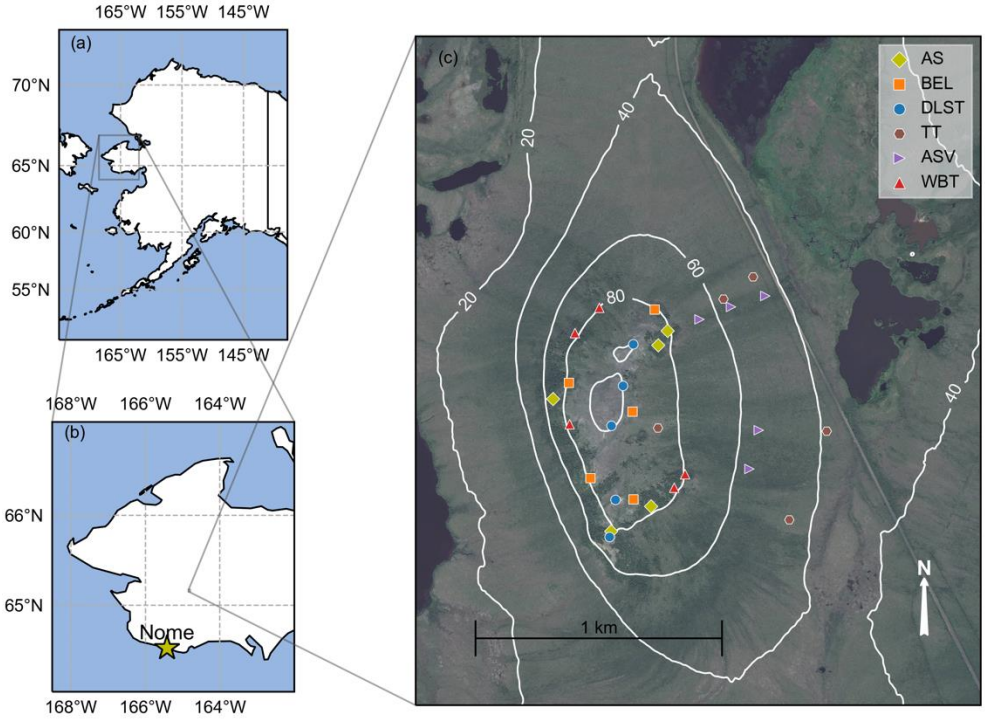

Figure 1: Location of Kougarok Hillslope field sites on the Seward Peninsula of Alaska, USA, at mile marker 64 on the Kougarok road north of Nome, Alaska (Iversen et al., 2017; data citation). Panel (c) shows visual imagery, elevation (m), and individual plot locations colored according to community type. See Table 1 for full community type names and definitions.

Vegetation data were collected at the peak of the growing season in mid to late July 2016 and 2017 at the NGEE Arctic Kougarok Hillslope field site located in the interior of the Seward Peninsula of Alaska (65°09'50.1"N, 164°49'34.2"W; Figure 1). The hillslope is comprised of an exposed, rocky outcrop with alpine vegetation at its summit surrounded by steep, well-drained slopes that transition to gently sloping alder savanna in water tracks and graminoid tussock-

lichen tundra in inter-water tracks, and then to lowland wet tundra. The hillslope spans a roughly 100 m change in elevation and a variety of plant communities are present across the varying topography (Figure 2). Alder shrublands are found along the well-drained slopes below the crest of the hill and are interspersed with patches of willow-birch and dwarf shrub lichen tundra. Extensive field site details are described in Salmon et al. (2019a).

We surveyed the six dominant plant communities along the hillslope, which varied in their shrub abundance, canopy height, and structure, to characterize the vegetation composition at the site following the recommended protocol of Walker et al. (2016) (Breen et al., 2020; data citation) (Table 1, Figs. 2, 3). Five replicate vegetation composition plots from each plant community were chosen subjectively in areas of homogeneous and representative vegetation and varied in size from 1-25 m^2 depending on canopy structure and height. The surveyed plot area was 1 x 1 m for all plant communities except for the taller stature willow-birch tundra (2.5 x 2.5 m) and alder shrubland (5 x 5 m). For each plot, all plant species (vascular plants, lichens, and bryophytes) were recorded along with visual estimates of their percent cover. For plots with multiple canopies, field cover estimates are absolute cover, meaning that the total cover per plot can be >100%. We calculated relative cover values (adding to 100%) from the field data and use these for all subsequent analyses. Plant species were further aggregated into nine PFTs based on growth patterns and plant traits (see Breen et al., 2020 dataset for a full species list with PFT designations). Biomass sampling plots were paired with a subset of vegetation composition plots distributed across the six dominant plant communities (Table 1), with two replicate plots per community.

Figure 2: Toposequence figure of the Kougarok hillslope showing the distribution of plant functional types and communities along with underlying soil layers. Vegetation and soil depths not drawn to scale. PFTs are listed that within each hillslope and the dominant PFTs (mean cover >15%) are indicated in bold. See Table 1 for full names and definitions of plant communities.

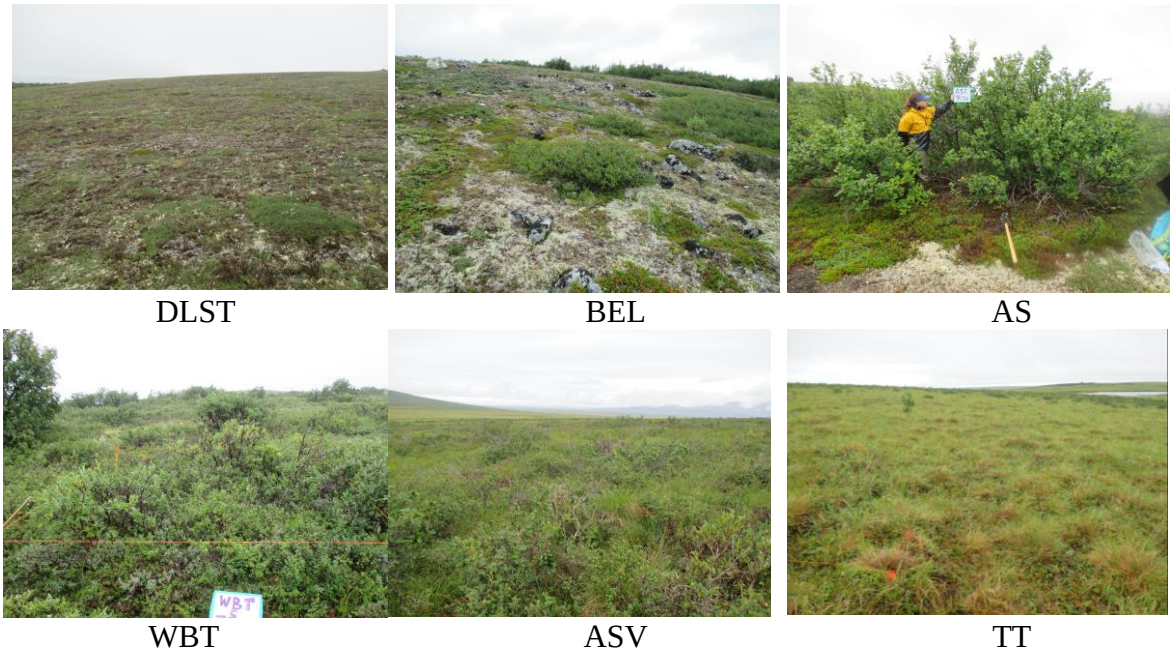

Figure 3: Representative photographs of the six plant communities. See Table 1 for full names and definitions.

For all deciduous low to tall individuals in the plots (*Alnus viridis* ssp. *fruticosa*, *Betula glandulosa*, *Salix alaxensis*, *S. glauca*, *S. pulchra*, and *S. richardsonii*) maximum shrub height and stem basal diameters were measured. We then performed a destructive harvest of one individual for each of the low-to-tall shrub species present in the plot to determine whether existing allometries could be applied. Following the destructive harvest of these low-to-tall shrub species, we separated attached dead leaves, inflorescences, live leaves, attached dead wood, live wood, and current year's stem growth. The dry aboveground biomass of harvested shrubs was within the range of published allometric relationships (see Supplementary Figure 1 and Berner et al., 2015). We consequently used Berner et al. (2015)'s allometric equations to determine aboveground biomass and NPP for the low to tall shrubs we surveyed but did not harvest. The allometric relationships in Berner et al. (2015), however, do not separate leaf biomass from stem biomass. To quantify leaf biomass, we applied the ratio of leaves to the sum of new leaves and stems observed in our harvest. The ratios in our data (0.80-0.87) were similar to values observed within a subset of the Berner et al. (2015) data (0.80, *personal communication*). We assumed leaf NPP for deciduous shrubs was equivalent to the entire leaf pool. Stem NPP is the sum of primary stem NPP (extension of new stem) plus secondary stem NPP (thickening of existing stems). Primary stem NPP was calculated as the NPP from Berner's allometric equations minus the leaf NPP. Secondary stem NPP was calculated based on ratios of secondary stem growth to primary stem growth observed for *Salix* and *Betula* at the Toolik Field Station Arctic LTER Site (Bret-Harte et al., 2002). The ratio applied to *Alder* (henceforth 'alder shrubs') was an average of *Salix* and *Betula*.

Aboveground biomass of understory vegetation was sampled using 20 cm × 50 cm clip plots (Salmon et al., 2019b). Understory species include bryophyte, lichen, graminoid, forb, and shrub PFTs (Table 1). All material from understory clip plots was cut at the level of the moss or soil surface and sorted by tissue type (stem versus leaf) and tissue age (current year versus older). Live moss was distinguished from dead based on color and live liverworts were combined

with live mosses as part of the bryophyte PFT. Net primary productivity was calculated based on new versus old tissues and leaf habit of the plant. Note that while deciduous dwarf shrubs were observed in plant survey plots, none occurred in biomass sampling plots.

Fine-root biomass and rooting depth distribution were measured on $n = 2$ soil cores collected within each of the biomass plots ($n = 2$ biomass plots per plant community) (Salmon et al., 2019c). In the field, 7.62-cm diameter soil cores were taken to the depth of rock or frozen soil and separated into depth intervals of roughly 10 cm. Soil depth was estimated using a thaw depth probe, noting whether the resistive layer the probe encountered was rock or frozen soil. Soil depth increments were frozen and shipped to ORNL for processing. In the lab, intact soil depth increments were divided in subsections where one subsection was used to determine soil properties and the other subsection was used to assess the biomass of living fine roots (<2 mm diameter). Roots were classified as live based on tensile strength and morphology. Fine roots could not be reliably attributed to specific species or PFTs, and fine-root biomass was therefore aggregated at the plot level for analyses. Fine-root production was estimated using community-specific, average lifespan estimates of fine-root populations from similar Arctic plant communities (Table S2).

Rhizome biomass and belowground stems were not directly measured because soil cores were not large enough capture their spatial variability, and aboveground surveys could not capture this belowground pool. Rhizome biomass was therefore estimated using relationships between aboveground biomass and rhizomes for PFTs and plant communities observed at Toolik Lake (Shaver & Chapin, 1991).

Leaf areas of understory clip plots and shrub harvests were measured by scanning entire leaves (WinRHIZO, Regent Instruments Inc., Quebec, Canada) or by taking leaf punches with a known diameter. Leaves and leaf punches were then dried and weighed so that leaf area and mass could be used to calculate Specific Leaf Area (SLA, cm^2/ g). Leaf, stem, and fine roots from understory clip plots, shrub harvests, and soil cores were dried, ground, and analyzed for %C and %N by weight on an elemental analyzer (Costech ECS 4010, Costech Analytical Technologies, Inc., Valencia, CA, USA).

All measured plant biomass, NPP, and tissue characterization data were aggregated over species to the PFT level. Each plant community was thus defined as an assembly of PFTs with the relative cover of each PFT varying by plant community. These relative covers were then used to drive community-specific simulations in ELM (see below).

Table 1: Kougarok Hillslope dominant plant communities. Observed soil depth indicates the measured depth to a resistive layer (Iversen et al., 2019a) and whether the resistive layer was rock or frozen soil. Note that in the model, soil depth to rock was assumed to be the level at which a thaw probe encountered primarily rocky material, or alternatively, the model maximum soil depth of 3.8 m if the probe reached frozen soil rather than rock. Measured depth to frozen soil was not used to configure model soil depth because ELM simulates thaw depth dynamically (Section 2.2).

CAVM Physiognomic Map Unit Name (Raynolds et al. 2019)	Plant Community Name	Brief description	Max observed vegetation height (cm)	Observed soil depth (cm)
Barrens and barren complexes: Areas with predominantly barren soils or bedrock, or covered by biological soil crusts but lacking much cover of vascular plants.				
Carbonate mountain complex; and more specifically prostrate dwarf-shrub, herb, lichen tundra at higher elevation	Dryas-lichen dwarf shrub tundra (DLST)	Dry tundra with patchy vegetation. Dominated at our site by *Dryas punctata* ssp. *alaskensis* (equivalent to *D. octopetala* ssp. *alaskensis*) and other prostrate dwarf shrubs with graminoids and forbs. Lichens are abundant. Occurs on the rocky, exposed outcrop at the summit and hillcrest.	23	10 (rock layer)
Graminoid tundras: Areas with tundra vegetation dominated by graminoid plants (sedges, grasses and rushes), mainly in mesic areas at high latitudes and ice-rich permafrost areas in the low Arctic.				
Tussock- sedge, dwarf-shrub, moss tundra	Tussock-lichen tundra (TT)	Moist tundra, dominated by tussock cottongrass (*Eriophorum vaginatum*) and dwarf shrubs. Mosses are abundant. Occurs along the backslope and footslope of the hill between water tracks.	38	33 (frozen layer)
Erect-shrub tundras: Areas with tundra vegetation dominated by erect dwarf shrubs or low shrubs and mosses mainly in mesic areas.				
Erect dwarf-shrub, moss tundra	Birch-Ericaceous lichen shrub tundra (BEL)	Moist tundra dominated by erect dwarf shrubs (*Betula nana, Empetrum nigrum, Arctous alpina, Kalmia procumbens*) and abundant lichens. Occurs on the hillcrest and shoulder of the hill.	27	26 (rock layer)

Low-shrub, moss tundra	Willow-birch tundra (WBT)	Moist acidic shrublands dominated by low to tall shrubs (*Salix* spp., *Betula nana, B. glandulosa*), dwarf shrubs and mosses. Occurs on the backslope of the hill.	146	32 (frozen layer)
	Alder savanna (ASV)	Moist tussock-lichen tundra with patches of alder (*Alnus viridis* ssp. *fruticosa*, < 2 m tall) and other low and dwarf shrubs. Occurs in water tracks on the lower backslope and footslope.	132	35 (frozen layer)
	Alder shrubland (AS)	Moist acidic shrublands on hillsides with closed low to tall alder (*Alnus viridis* ssp. *fruticosa*) canopies. Low and dwarf shrubs are also abundant. Occurs on the upper backslope in a band below the hillcrest and shoulder of the hill.	320	20 (rock layer)

2.2 Default land model description

The E3SM Land Model (ELM) is the land surface component of E3SM. ELM simulates water, energy, C, N, and P cycles in terrestrial ecosystems. Here, we briefly describe model processes relevant to this study. For additional model description, see (Burrows et al., 2020; Ricciuto et al., 2018; Yang et al., 2019). ELMv1 branched from CLM4.5 (Oleson et al., 2013, equivalent to ELMv0), and incorporates new developments including P cycling (Yang et al., 2019). C, N, and P cycles are simulated in vegetation and soil organic matter. Vegetation is divided into multiple PFTs with independent parameterizations controlling photosynthesis, leaf gas exchange, biomass allocation, and other processes. Biomass growth allocation among different tissues is based on fixed allocation ratios relating leaf, fine-root, aboveground woody tissue (stem), and belowground woody tissue (coarse-root) growth fractions. Woody tissues are divided into living (e.g., respiring sapwood) and dead (e.g., non-respiring heartwood) fractions. Plants are divided into tree, shrub, and non-woody types. Trees and shrubs both have woody tissues but use different calculations for biomass allocation to woody tissue and different allometric parameters for calculating canopy height. Non-woody PFTs in the default model are assumed to have only leaves and fine roots. Each PFT also has nonstructural storage pools for C, N, and P. Deciduous plants use these nonstructural pools to grow leaves and fine roots in the spring, and to store C and nutrient uptake in nonstructural pools during the growing season for use in the next season. The fraction of nonstructural C and nutrient pools used each spring season by deciduous plants is set to 50% in the default model configuration. Evergreen plants in the unmodified model grow biomass throughout the growing season in connection with current photosynthesis, with nonstructural pools used only under nutrient-limited conditions. Maintenance respiration of living tissues (including leaves, fine roots, and living woody tissue) is a function of tissue N content and modified by a Q10 temperature dependence. Leaf respiration is assumed to stop when plants are under snow, but root respiration does not include a dormancy factor in the default ELMv1 model configuration. ELM simulates energy and water dynamics in soil including liquid and frozen water content and dynamic active layer thickness.

2.3 Model changes

2.3.1 Soil depth to bedrock

ELM uses a default soil depth to bedrock of 3.8 m. Roots, water flow, and soil biogeochemistry are only simulated in layers above the bedrock depth. In addition to the bedrock layer, ELM simulates a dynamic active layer thickness (ALT) at sites underlain by permafrost as the deepest thawed layer in the modeled soil temperature profile. Plant roots in the model are not permitted to grow deeper than the maximum active layer thickness from the previous growing season. Measured soil depth to rocky layers varied substantially across vegetation communities (Table 1). The DLST community in particular had very shallow soils and significant areas of exposed rock. For this study, ELM was configured to use measured soil depth to the rocky layer as depth to bedrock in plant communities with shallow rocky layers to test the importance of this abiotic site factor in simulated biomass and NPP; for the purposes of this analysis, those communities were DLST, BEL, and AS (Table 1). For model simulations, soil depth to rock was assumed to be the level at which a thaw depth probe encountered primarily rocky material, or the model

maximum soil depth of 3.8 m if depth probes reached frozen soil rather than rock. Measured depth to frozen soil was not used to configure model soil depth because ELM simulates thaw depth dynamically. Model active layer thickness was not modified based on site measurements.

2.3.2 PFT changes

Default ELM PFTs are based on broad groups relevant for global-scale configurations (Wullschleger et al., 2014). These include one broadleaf deciduous boreal shrub PFT and one C3 arctic grass PFT that was assumed to be annual, allowing leaves and fine roots to senesce at the end of each growing season. No non-vascular PFTs (lichens or bryophytes) were included in the default ELM PFTs. To match the observed plant diversity at the Kougarok Hillslope field site, we defined new ELM PFTs based on literature and site measurements and altered model functionality to match observed Arctic plant traits (Table 2). The original model's deciduous broadleaf boreal shrub was divided into five different shrub types, representing the diversity of leaf habits (both evergreen and deciduous types occur at the Kougarok Hillslope site) and differences in growth patterns including potential maximum height and aboveground-belowground partitioning. Dwarf prostrate shrubs, such as *Salix arctica*, reach a maximum height of 10 cm, while dwarf erect shrubs are <40 cm tall. Low shrubs vary from 40 cm to 2 m in height. Low-to-tall shrubs can potentially reach over 2 m in warmer microsites depending on growing conditions. Deciduous low to tall shrubs were further divided into alder and non-alder (willow and birch) PFTs. Alder was separated from other low to tall shrubs because it hosts N-fixing actinomycetes in its root nodules and has significantly different tissue chemistry, particularly higher leaf N concentrations. Development and evaluation of new alder N fixation capabilities was beyond the scope of this paper, but ecosystem-scale N fixation rates in the alder-dominated AS plant community were increased in our simulations to ensure that simulated plant growth in the community dominated by N fixers would not be N limited, as consistent with observations of an open N cycle in the AS community (Salmon et al., 2019a).

The new PFTs were parameterized using biomass measurements from the Kougarok Hillslope site (Salmon et al., 2019b). Parameterization was focused on biomass rather than height because canopy height in ELM is calculated from aboveground biomass using fixed allometric parameters and is used primarily for calculating atmospheric roughness rather than directly affecting C and nutrient cycling. Tissue allocation parameters (leaf to fine-root growth ratios and stem to leaf growth ratios) were the primary parameters that were adjusted. Leaf maximum photosynthesis rate (VCmax) is calculated in ELM using leaf N content (a static PFT parameter) and the fraction of leaf nitrogen in the Rubisco enzyme (FLNR) parameter. Leaf N content was parameterized using site measurements, and FLNR was adjusted so that growing season VCmax matched literature values for Arctic PFTs (Bubier et al., 2011; Nash et al., 1983; Rogers et al., 2017; Williams & Flanagan, 1998). Specific leaf area for each PFT was parameterized using site measurements. Rooting depth distribution in ELM follows the double-exponential formulation of Zeng et al., (2001), which uses two depth parameters. These parameters were adjusted based on maximum rooting depth of arctic plant species reported by Iversen et al. (2015). Rooting depth is further constrained in the model by adjusting root depth distribution so it does not extend below the depth to bedrock or deeper than the thickness of the simulated active layer.

Graminoids (including grasses, sedges, and rushes) are assumed to be deciduous or annual plants in the default E3SM configuration, allowing all leaf and fine root biomass to senesce each autumn and regrow in the spring. However, the majority of Arctic graminoids have leaf and fine root tissues that persist for multiple growing seasons (Shaver & Laundre, 1997).

Therefore, graminoids in the new Arctic PFT configuration were set to be evergreen plants, with a leaf lifespan of two years (Shaver & Laundre, 1997) and a fine-root lifespan of approximately 3 years (Sullivan et al., 2007). Forbs, including non-flowering vascular plants such as ferns and horsetails, which were more likely to be truly deciduous at the Kougarok Hillslope site, were separated from graminoids and remained deciduous in the updated model.

Many arctic plants allocate a high fraction of their growth to belowground tissues (Iversen et al., 2015), and grow a relatively small amount of new leaf and fine-root tissue each year, reflecting a conservative growth strategy consistent with short growing seasons (Thomas et al., 2020). Thus, arctic PFTs were adjusted to maintain larger storage pools and express a lower fraction of storage into tissue growth each year. In the original ELM configuration, non-woody plants were limited to include only leaf, fine-root, and storage pools. The model was modified to add rhizome tissues, treated as living coarse-root tissue, to graminoids and forbs (woody shrub PFTs in the model already have associated coarse roots). Allocation to coarse root and rhizome tissues were parameterized using site estimates of rhizome and belowground stem biomass.

Bryophytes and lichens were introduced as separate PFTs. While nonvascular plants and lichens differ in many important ways from vascular plants, including in their water transport, transpiration, and photosynthesis capabilities, development of new nonvascular-specific processes was beyond the scope of this study. Instead, nonvascular PFTs were parameterized as nonwoody plants with very low root biomass and photosynthesis parameters were set based on previous measurements of moss and lichen photosynthetic capabilities (Nash et al., 1983; Williams & Flanagan, 1998).

Fine-root respiration in ELM is a function of fine-root N concentration and also depends on temperature through a Q10 relationship. The default model does not allow living roots to become dormant during the winter. To prevent fine-root respiration from depleting plant C reserves over the long winter season, the model was modified to allow fine roots to become dormant when soil temperatures were below -1 ºC (Monson et al., 2006). In a dormant state, fine-root respiration was reduced to 5% of its non-dormant rate.

Table 2: PFTs and key parameters. FLNR: Fraction of nitrogen in Rubisco. Model max rooting depth is defined as depth that 99% of root biomass is above, calculated from the rooting depth parameters. Data sources used to determine the new value of each parameter are shown as letters in the bottom row with citations in the footnote.

PFT	Root:leaf allocation ratio	Stem:leaf allocation ratio	Coarse root:stem ratio*	Leaf C:N	Fine root C:N	FLNR	Specific leaf area (cm^2 g C^{-1})	Leaf habit	Rooting depth params (m^{-1})	PFT max rooting depth (cm)
Default PFTs (Simulations 1 and 2)										
Broadleaf deciduous boreal shrub	2.0	0.2	0.3	25	42	0.1365	300	Deciduous	7.0, 1.5	260
C3 arctic grass	2.0	N/A	N/A	25	42	0.1365	300	Deciduous	11.0, 2.0	200
New PFTs (Simulation 3)										

Lichen	0.2	N/A	N/A	84	42	0.435	300	Evergreen	400, 800	0.98
Bryophyte	0.1	N/A	N/A	55	42	0.485	300	Evergreen	100, 200	3.9
Evergreen dwarf shrub	3.0	0.1	1.0	44	58	0.0755	134	Evergreen	30, 13	30
Deciduous dwarf shrub	1.5	0.2	0.5	27	58	0.1365	213	Deciduous	13, 10	42
Deciduous low shrub	1.4	0.2	0.5	31	58	0.1365	201	Deciduous	13, 10	42
Deciduous low to tall shrub	1.3	0.2	0.5	22	58	0.1365	237	Deciduous	13, 10	42
Alder shrub	0.25	0.5	0.6	21	58	0.1365	275	Deciduous	13, 10	42
Forb	1.5	N/A	0.1*	30	58	0.2	300	Deciduous	11, 9	47
Graminoid	4.0	N/A	0.1*	27	75	0.09	165	Evergreen	11, 9	47
Data source for new parameterization	a, b	a	c	a	b	d	a	N/A	b	b

*For graminoids and forbs, rhizome-leaf ratio is shown in the coarse root/stem ratio column
a. (Salmon et al., 2019b)
b. (Salmon et al., 2019c)
c. (Shaver & Chapin, 1991)
d. Bubier et al. (2011); Nash et al. (1983); Rogers et al. (2017); Williams & Flanagan (1998)

2.4 Model simulations

ELM simulations were conducted for the Kougarok Hillslope site using meteorological driving data from the Scenarios Network for Alaska and Arctic Planning (SNAP) downscaled climate projection dataset using NCAR-CCSM forcing (Bieniek et al., 2020 dataset; Walsh et al., 2018). Model simulations were spun up using 200 years of accelerated decomposition, followed by 600 years of regular spinup (Koven et al., 2013; Thornton & Rosenbloom, 2005). The SNAP forcing included the historical period from 1970 to 2005, extended through 2100 using the RCP8.5 scenario. Spinup and historical simulations were conducted beginning in 1850, with periods prior to 1970 simulated by repeating the historical period of the SNAP forcing. SNAP meteorology was bias corrected to match DAYMET precipitation at the site, with winter precipitation reduced by a factor of 2 to better match estimates of snow depth and spring snowmelt date at the site. Atmospheric CO_2 forcing used historical time series data starting in 1765 and extending through 2100 using the RCP8.5 scenario.

All simulations were repeated using three levels of model simulations representing a progression from the default model configuration of ELM within E3SM to a specific parameterization of Arctic PFTs within an updated ELM (Figure 4). Simulation 1 used grid cell

data from a global E3SM configuration, including the fractional area of E3SM PFTs assigned to the grid cell containing the Kougarok Hillslope site in global simulations. This simulation did not distinguish between different plant communities on the Kougarok Hillslope, but instead used a single point simulation to represent the entire area. Simulation 2 used default E3SM PFT definitions combined with adjusted depth to bedrock for plant communities with shallow rocky layers to represent the role of abiotic soil factors in driving site differences, and adjusted the relative areas of the broadleaf deciduous boreal shrub and C3 arctic grass PFTs to reflect the observed spatial coverage of shrub and non-shrub PFTs across Kougarok Hillslope plant communities. Areas of all non-shrub PFTs, including graminoids, forbs, lichens and bryophytes, were included in the C3 arctic grass coverage fraction for this simulation. Simulation 3, the most site-specific level, used the new arctic PFT definitions and parameterizations based on the vegetation types present at the site, including measured soil depths in communities where soil was underlain by rocky layers (Table 2). While relative spatial areas of PFTs varied among plant communities, the parameters of each PFT were the same regardless of plant community.

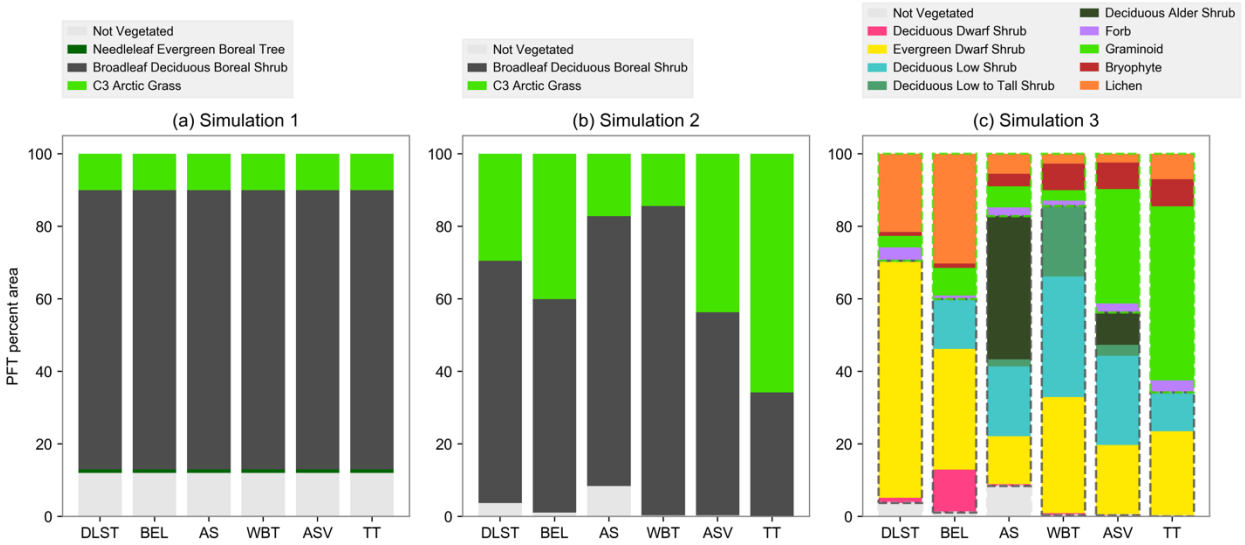

Figure 4: Relative areas of PFTs for three model configurations. (a): Downscaled E3SM grid cell and E3SM PFTs (Simulation 1); (b): E3SM PFTs with community-specific fractions of shrub, grass, and non-vegetated areas (Simulation 2); (c): Measured areas of Arctic PFTs (Simulation 3). Dashed outlines show which arctic PFTs were combined into the PFT areas in Simulation 2.

3 Results:

3.1 Contemporary vegetation biomass patterns

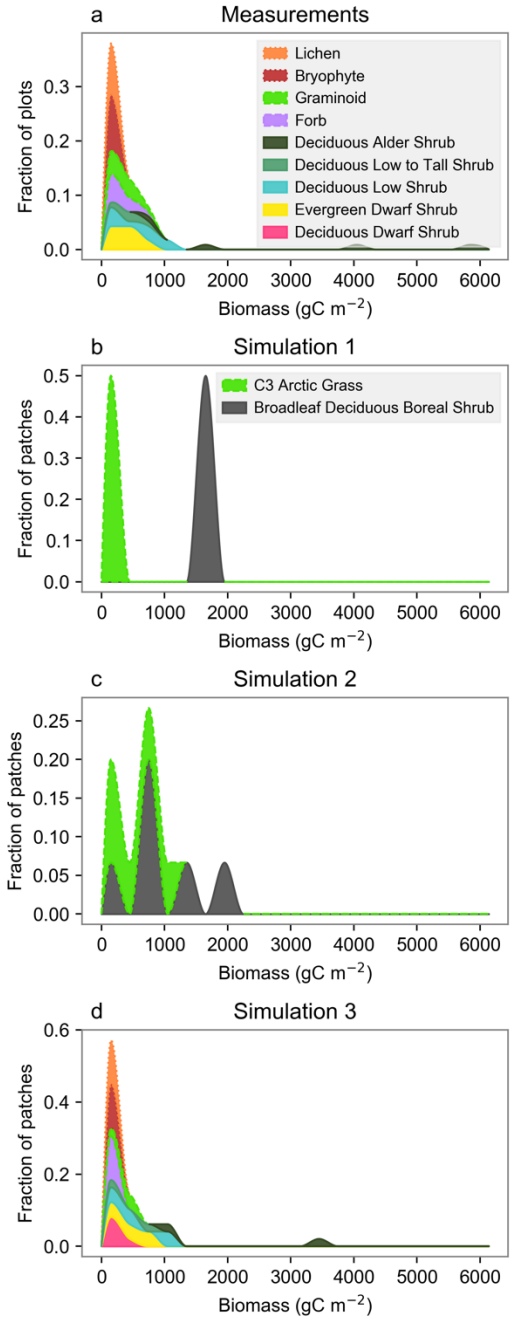

Figure 5: Smoothed histograms of vegetation biomass distribution, color coded by PFT. (a): Observed PFT biomass. (b): E3SM grid cell with default PFTs and single soil depth (Simulation 1). (c): E3SM PFTs with varying soil depths and relative areas of shrubs and grasses (Simulation 2). (d): Arctic PFTs with varying soil depths (Simulation 3).

Distributions of measured PFT biomass among plots highlighted the diversity of PFTs present along the Kougarok Hillslope gradient (Fig. 2) as well as the variability in their contributions to plot biomass (Fig. 5a). Measurements showed that various dwarf and low shrub PFTs contributed a range of biomass values across measurement plots, from less than 100 g C m^{-2} to over 1000 g C m^{-2}. Low to tall deciduous non-alder shrubs also tended to make small contributions (less than 1000 g C m^{-2}) to total plot biomass despite their larger stature. Only alder shrubs dominated plots with high biomass of greater than 1500 g C m^{-2}, with the most productive alder plots dwarfing other PFTs with up to 6000 g C m^{-2}. Forbs and graminoids ranged up to 1000 g C m^{-2}. Nonvascular PFTs, including bryophytes and lichens, generally had low total biomass but were widespread among plots.

Distributions of simulated PFT biomass (averaged from years 1990-2010, following spinup and historical period simulations) across modeled plant communities showed how adding information to the model improved both diversity and biomass of modeled relative to observed PFTs. Simulations using original E3SM PFTs (Simulation 1; Fig. 5b) showed how a grid-cell-level simulation with only two PFTs led to underestimates of biomass variability across plots. These simulations overestimated shrub biomass compared to measurements and missed the significant fraction of plots with small amounts of shrub biomass or moderate amounts (> 500 g C m^{-2}) of non-shrub biomass. When variations in soil depth to bedrock and relative shrub and graminoid area were taken into account (Simulation 2; Fig. 5c), simulated variability in shrub biomass was improved relative to observations, with some low-biomass plots represented. However, Simulation 2 still overestimated the prevalence of shrub biomass in the 1000-2000 g C m^{-2} range while not reproducing high-biomass alder plots. Simulated biomass using new ELM arctic PFTs parameterized with site-level observations (Simulation 3; Fig. 5d) had distributions of PFT biomass that were more consistent with observations for nonvascular PFTs, graminoids, forbs, and most shrubs. However, the modeled biomass was skewed somewhat low and underestimated biomass of forbs and dwarf shrubs in communities where they reached higher biomass (in the 500-1200 g C m^{-2} range). The model also failed to reproduce the highly-productive alder sites, with modeled alder biomass occurring mostly in the 1500-2000 g C m^{-2} range compared to observed alder biomass of up to 6000 g C m^{-2}.

Patterns of biomass were clarified by separating the study area into representative plant communities for comparison with modeled plant communities (Figure 6). Measured biomass in the DLST community at the summit and crest of the hillslope was dominated by lichens, with evergreen dwarf shrubs contributing a small amount despite their larger fractional cover (Fig. 6a). The BEL community at the shoulder of the hillslope (Fig. 6b) also had a large fraction of biomass made up by lichens, but dwarf and low shrubs made up a larger fraction of aboveground biomass, and also contributed to a substantial amount of belowground biomass. The tall-statured AS community, predominantly on the upper backslope, had the highest biomass of any community due to dominant alder shrubs (Fig. 6c). The WBT community, also on the backslope, was dominated by deciduous shrubs, with biomass divided relatively evenly between low and low to tall shrubs (Fig. 6d). The ASV community on the lower backslope and footslope had lower biomass of shrubs than AS and a higher fine-root biomass relative to aboveground biomass (Fig. 6e). Biomass of the TT community on the footslope was dominated by graminoids, specifically tussock-forming sedges. Biomass in this community was largely belowground, with fine roots making up a large fraction of total biomass (Fig. 6f).

Model simulations using default E3SM grid cell PFTs for the grid cell containing the Kougarok Hillslope site (Simulation 1) were dominated by deciduous shrubs. This pattern was most consistent with the AS and WBT plant communities but did not reflect the diversity of shrub growth patterns in those communities. The other communities did not match the E3SM grid cell pattern well, including DLST, where the default model greatly overestimated shrub biomass, and the ASV and TT communities, where the default model underestimated the coverage and biomass of graminoids. Simulations with community-specific soil depths and relative cover of grasses and shrubs (Simulation 2) were somewhat improved relative to observations, with improved model estimates of total biomass in the DLST and BEL communities. However, these simulations greatly underestimated biomass in the AS community. In addition, E3SM PFTs (Simulations 1 and 2) substantially underestimated the belowground fraction of total biomass (including rhizomes and fine roots) in all plant communities except the nonvascular-dominated DLST community, which had very low belowground biomass. Simulation 3, with measurement-constrained tundra PFTs, corresponded well with observations, although alder biomass in AS and lichen biomass in DLST were still underestimated.

Soil depth to bedrock in the model was an important control on vegetation biomass, as evidenced by the contrast between Simulations 1 and 2. While soil depth for communities underlain by rocky layers (DLST, BEL, and AS; Table 1) was set to measured values, active layer thickness (the primary control on plant-available soil thickness in WBT, ASV, and TT) was determined by ELM thermal-hydraulic calculations. Mean maximum active layer thickness simulated in ELM over the 1990-2010 period was 2.3 m, 4.6 m, and 12.6 m respectively for the WBT, ASV, and TT communities. These depths were roughly an order of magnitude greater than observed depths to frozen layers of 32-33 cm for those communities (Table 1).

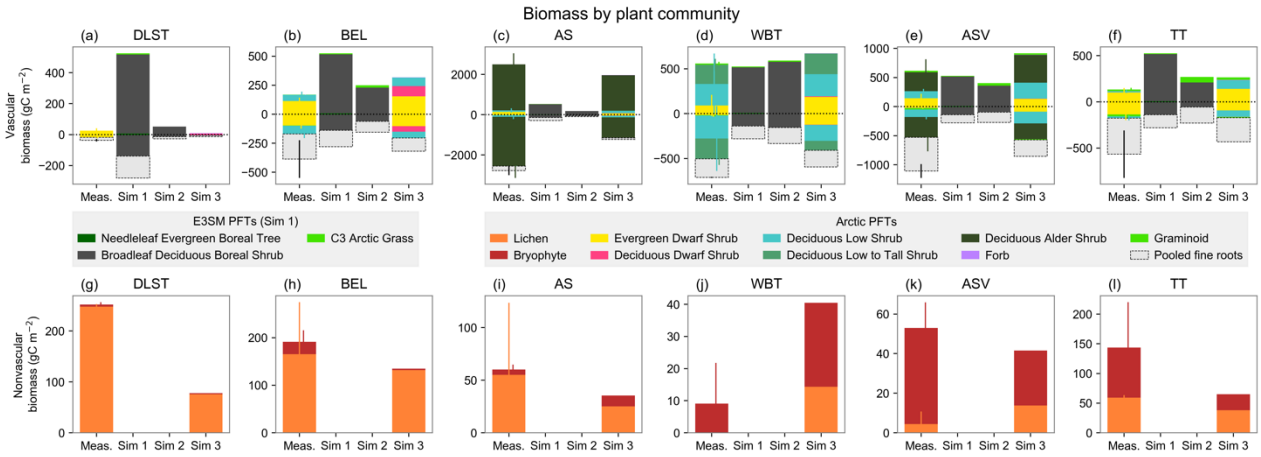

Figure 6: Total biomass in each plant community. Panels a-f show vascular biomass and panels g-l show nonvascular biomass. Aboveground biomass is shown as upward bars, and belowground biomass (including PFT-specific rhizomes and pooled fine roots) is shown with downward bars. Sim 1: E3SM grid cell data. Sim 2: E3SM PFTs with community-specific shrub/grass relative areas and soil depth to bedrock. Sim 3: Arctic PFTs and community composition. Note that simulations 1 and 2 lacked nonvascular PFTs. Colors in each bar indicate the biomass of different PFTs. Error bars show standard deviation of measurements of each PFT. Note that vertical scales vary among panels.

Comparing the biomass of individual PFTs between model simulations and measurements highlighted the improvements from Arctic-specific PFT developments (Figure 7). Individual shrub PFTs in Simulation 3 generally reproduced variations in biomass across plant communities (R^2 = 0.32 and 0.7 for evergreen dwarf shrub and deciduous low shrub, respectively; only two data points were available for tall and alder shrubs; Fig. 7c-f). Simulation 2, by contrast, greatly underestimated biomass in the AS community leading to low correlation across communities (Fig. 7a; R^2 = 0.002). While the C3 arctic grass PFT in Simulation 2 did capture most of the observed variability in nonwoody vascular biomass (Fig. 7b; R^2 = 0.75), nonvascular PFTs were not defined in that simulation. In Simulation 3, graminoid biomass generally reproduced observations (Fig. 7g; R^2 = 0.87). Simulated forb biomass (Fig. 6h) was not as well correlated with observations (R^2 = 0.17), although total biomass of forbs was low compared to other PFTs. Simulated lichen and bryophyte biomass (Figs. 7j,i) both compared fairly well with observations, with a higher correlation for lichens, which also made up more total biomass (R^2 = 0.61 and 0.35 for lichens and bryophytes, respectively).

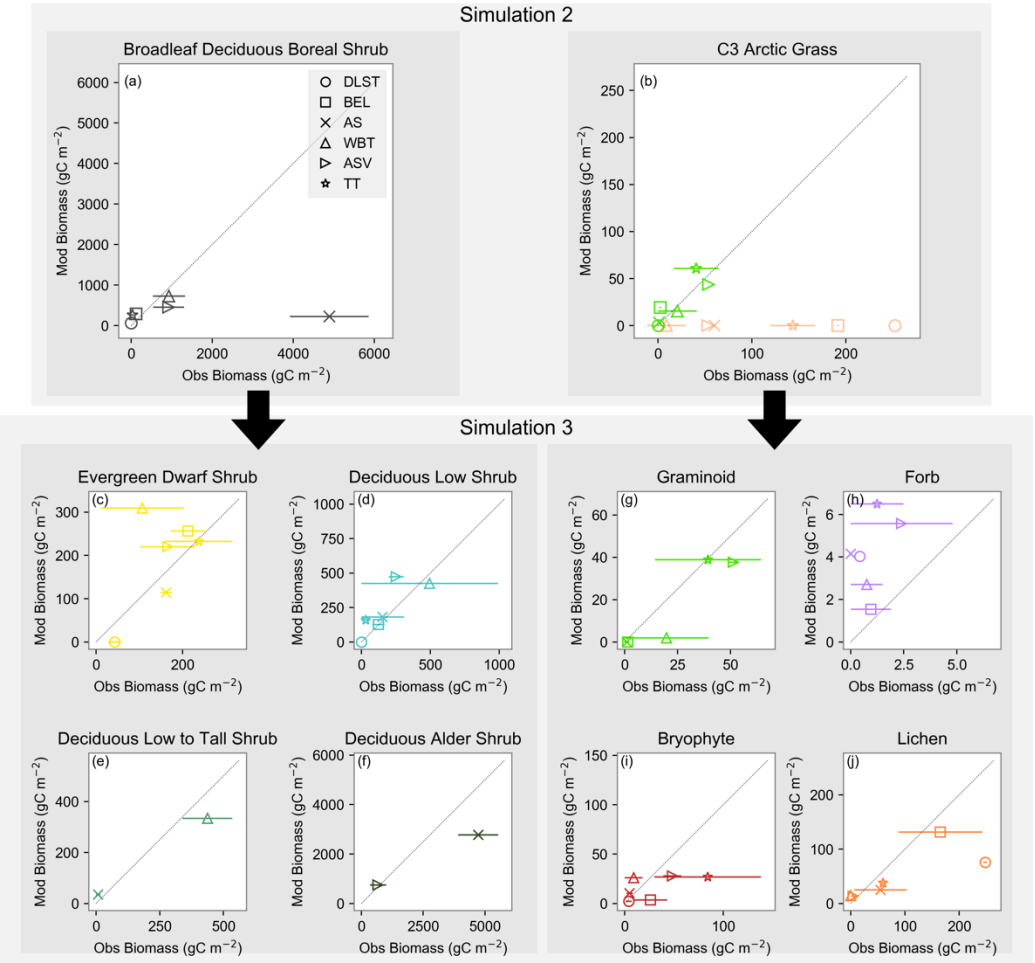

Figure 7: Modeled and measured biomass of each PFT. Different symbols show the different plant communities. Panels (a) and (b) show E3SM PFTs with site-specific soil depth and relative areas (Simulation 2) compared with observed PFTs pooled into shrub, non-shrub, and nonvascular groups. Panels c-j show new arctic PFTs (Simulation 3) compared with measured biomass of each PFT. Deciduous dwarf shrubs are not shown because biomass was not

measured for that PFT. Observed values show the mean of two plots, with a bar showing the range between the two measurements. Total measured nonvascular biomass is shown in orange symbols in the C3 Arctic Grass panel (b).

3.2 Historical and projected biomass changes

Time series of vegetation biomass showed clear historical patterns with substantial differences among the three simulations (Figure 8). All simulations showed gradual biomass accumulation over the historical period, followed by accelerating biomass accumulation from 2000 through 2080. However, different approaches to defining PFTs and communities drove large differences in historical and projected biomass across the hillslope's plant communities. Shallow depth to rocky layers in DLST and AS (Table 1) caused both historical biomass and projected biomass accumulation to be much lower in Simulation 2 than in Simulation 1. New, Arctic-specific PFTs (Simulation 3) drove dramatically larger biomass in shrub-dominated ecosystems for simulation 3 versus 2. These increases were especially notable in AS and ASV where N limitation was alleviated by higher N fixation associated with the alder shrub PFT included in Simulation 3.

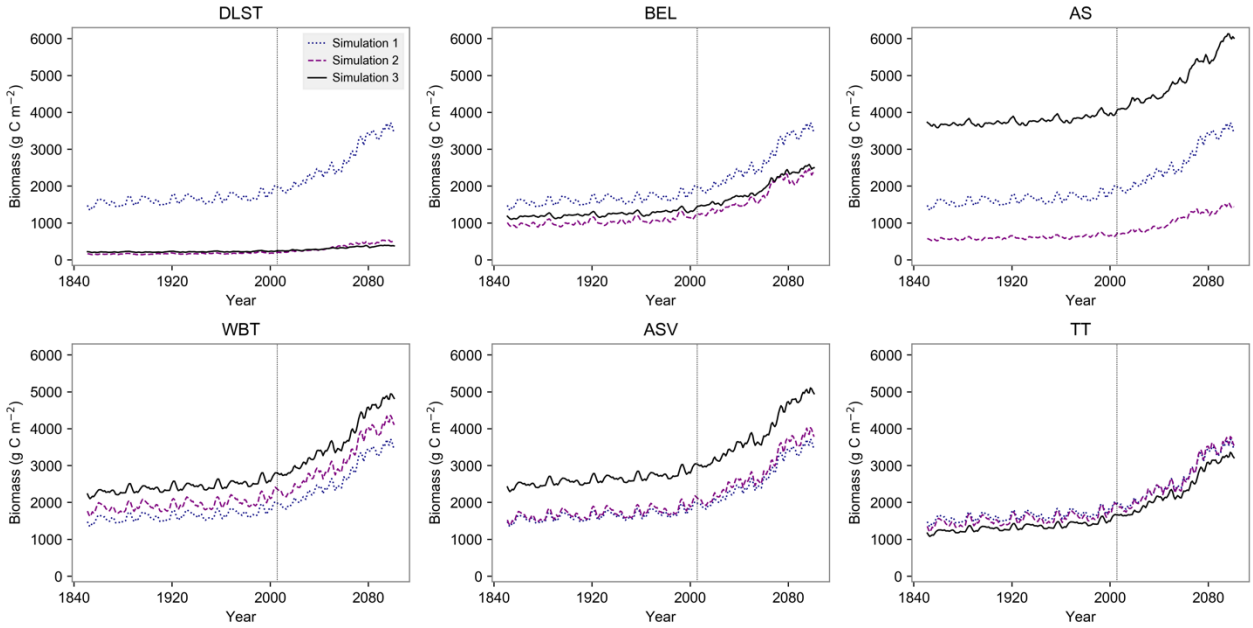

Figure 8: Time series of total community vegetation biomass for the three simulations. Vertical line indicates transition from historic to future climate drivers.

Changes in the biomass of individual arctic PFTs over time showed varying patterns across simulated PFTs and plant communities (Figure 9). Generally, biomass of mosses and lichens was less sensitive than that of vascular plants to changing climate and CO_2 concentrations, except in the lichen-dominated DLST community where lichen biomass increased significantly from 2000-2100. Low shrubs and graminoids had higher biomass growth responses than other PFTs in communities containing significant biomass of both graminoids and shrubs such as TT and ASV. This included alder in ASV, where it was eventually overtaken by low shrubs in terms of total biomass. In the AS community, however, alder had strong projected growth that drove community biomass accumulation from 2000-2100.

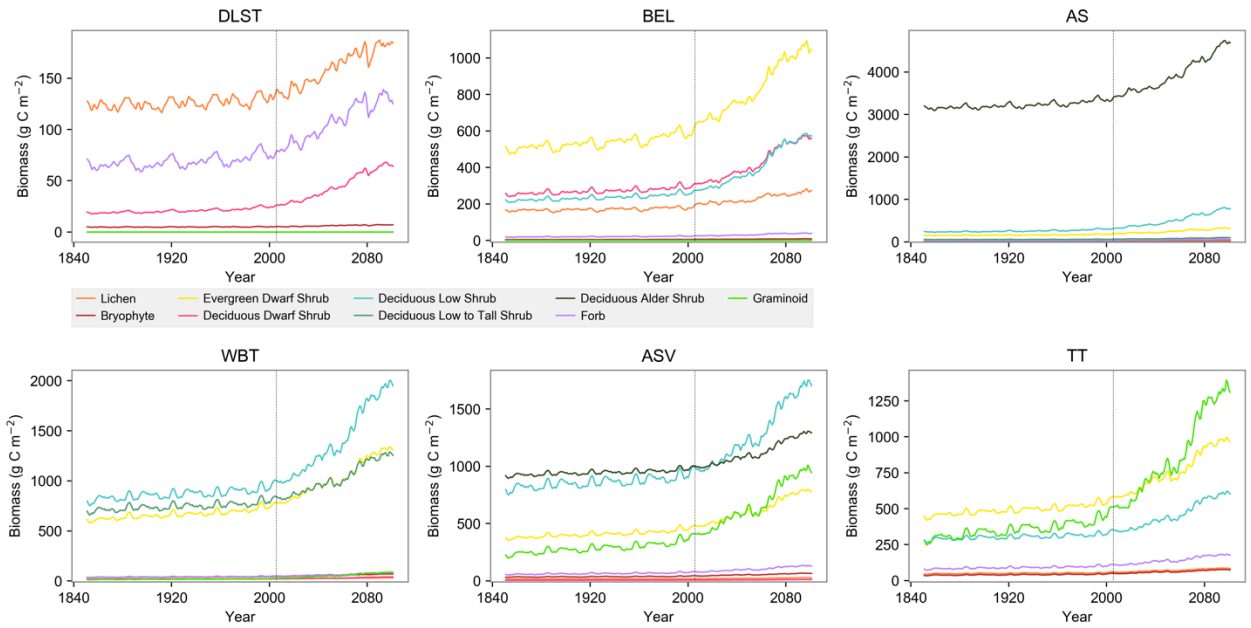

Figure 9: Time series of biomass of each PFT in Simulation 3 across the Kougarok Hillslope gradient of plant communities.

4 Discussion:

Tundra ecologists have long known that the diversity of plant species and functional traits across the Arctic tundra have important consequences for the cycling of energy, water, carbon and nutrients (Bjorkman et al., 2018; Bliss et al., 1981; Chapin et al., 1996; Sturm et al., 2005; Turetsky et al., 2012; Wielgolaski, 1972). By confronting a land surface model with site-scale measurements of plant biomass and tissue traits, above- and belowground, across a range of plant communities and functional types, we were able to identify deficiencies in the default model and improve representation of both plant functional type diversity and total values of biomass, above- and belowground, across a gradient of tundra plant communities on the Seward Peninsula of Alaska. Because it was limited to coarsely-defined boreal shrub and C3 arctic grass PFTs, the default model configuration in ELM failed to reproduce the diversity of plant traits and growth forms, which included several shrub forms, nonvascular lichens and bryophytes. Our model improvements highlight the importance of representing the diversity of Arctic plant growth forms, which have been previously identified as a challenge for traditional functional type approaches (Thomas et al., 2019; Wullschleger et al., 2014). Averaging over variation in Arctic PFTs has been shown to bias simulated biomass (Epstein et al., 2001), and our results were consistent with this finding. Even for species that mapped easily onto existing model PFTs such as low to tall shrubs and graminoids, the default model parameterization underestimated belowground biomass allocation, suggesting that current model simulations at global or pan-Arctic scales may underestimate belowground productivity despite overestimating the available rooting zone in several communities. Because a large proportion of soil organic matter is root-derived (Jackson et al., 2017; Rasse et al., 2005), this could lead to bias in simulated soil carbon stocks and should be revisited in large-scale model configurations. Previous analyses have shown that leaf photosynthetic traits are also often poorly parameterized in land surface models, particularly for arctic vegetation (Rogers, 2014; Rogers et al., 2017).

The large contribution of nonvascular bryophytes and lichens to total biomass in several of the plant communities in this study (Fig. 5) highlights the need for integration of these organisms into land surface models in the Arctic. Mosses, and particularly *Sphagnum* spp., play important roles in high-latitude ecosystems, including buffering the soil from air temperature fluctuations and potential permafrost thaw, forming a barrier to surface water fluxes, and influencing nutrient availability and ecosystem responses to fire (Beringer et al., 2001; Blok et al., 2011; Gornall et al., 2007; Kellner, 2001; Turetsky et al., 2012). Lichens can contribute significantly to C uptake and N fixation in arctic ecosystems (Crittenden & Kershaw, 1978; Lange et al., 1998) and play important ecological roles including forming an essential part of the caribou diet in the winter (Longton, 1997). While some large-scale models have begun to integrate nonvascular PFTs and their particular traits (e.g., Druel et al., 2019; Shi et al., 2020), ELM has, until now, lacked specific capability for nonvascular arctic PFTs. In this study, bryophytes and lichens were implemented within the existing PFT framework as nonwoody plants with very low belowground biomass. However, this approach does not incorporate the physiological differences that separate bryophytes and lichens from vascular plants, including water transport and lack of stomatal control, and as a result likely underestimates the differences in land-atmosphere energy and water fluxes in nonvascular-dominated communities compared to vascular-dominated communities (Porada et al., 2016; Stoy et al., 2012). More model improvements are needed to accurately represent bryophyte and lichen physiology in ELM. To this end, *Sphagnum* physiological processes such as capillary wicking of water and coupling of photosynthetic rate to tissue water content are being developed in ELM for northern peatland ecosystems (Shi et al., 2020), and these developments could be incorporated into arctic bryophyte simulations in the future.

Our simulations suggested that potential for future biomass accumulation varied greatly by plant community. Shrub-dominated communities as well as the graminoid-dominated TT community had strong biomass responses to warming and increasing atmospheric CO_2 levels, with biomass increasing by up to a factor of two, or up to 2 kg C m^{-2}, through 2100. In the shallow-soil, lichen-dominated DLST community, total biomass accumulation was low due to a combination of PFT traits that limited growth and shallow soils that limited water and nutrient availability. However, our simulations greatly overestimated active layer thickness in the three communities underlain by deeper soils. This could have biased the results toward greater growth potential in those communities by overestimating potential maximum rooting depth and access to water and nutrients. Even so, our simulated active layer thicknesses of greater than 2 m were consistent with previous large-scale model simulations in the Seward Peninsula region (Koven et al., 2011). These results highlight the importance of including landscape-scale variation in both abiotic factors, including lateral thermal-hydraulic processes, and plant communities in simulations of Arctic biogeochemistry. Simulations using a single average community across the grid cell omitted both the high and low ends of the biomass response distribution, which could introduce bias into larger-scale simulations of Arctic responses to global changes. Model overestimates of active layer thickness suggest that additional work is needed to improve permafrost thermal-hydraulic process representation in order to reduce potential bias in plant growth for permafrost-affected plant communities.

The enhanced vegetation growth in our simulations of arctic ecosystems under warming climate and increasing CO_2 concentrations is consistent with previous vegetation measurements (Myers-Smith et al., 2019), model simulations (Koven et al., 2011; McGuire et al., 2012) and evidence from remote sensing (Jia et al., 2003). The magnitude of biomass gains over the 21st

653 century in Simulation 1 was approximately 1.7 kg C m^{-2}, which was within the range of multiple
654 models applied to the Arctic region (Ito et al., 2016), and was consistent with an estimated 20%
655 increase in aboveground phytomass in circumpolar Arctic tundra from 1980-2010 (Epstein et al.,
656 2012). Taking into account heterogeneity in soil depths and plant communities (Simulation 3)
657 greatly expanded the range of biomass changes, from a gain of only 0.158 kg C m^{-2} in DLST to
658 an increase of approximately 2 kg C m^{-2} in the AS and WBT communities. This variability is
659 consistent with more detailed measurements and model simulations of changes in arctic
660 ecosystems. Myers-Smith et al. (2020) suggest that observed "greening" of the Arctic is
661 complicated by heterogeneity in ecological and physical factors. Shaver & Chapin (1991) noted
662 the large variation in biomass and primary production among tundra vegetation types within a
663 relatively small area, and Euskirchen et al. (2009) found that biomass change over the 21st
664 century in arctic ecosystems varied substantially between shrub- and sedge-dominated tundra
665 types. Epstein et al. (2001) found that multiple arctic PFTs were necessary to accurately
666 represent biomass and primary production in tundra ecosystems. Landscape factors such as
667 nutrient availability, water flow, disturbance history, growing season length, and presence of
668 competitors can have important effects on shrub expansion (Bhatt et al., 2017; Myers-Smith et
669 al., 2011, 2020). Similarly, Elmendorf et al. (2012) found that responses of different arctic PFTs
670 to warming varied with moisture and permafrost status, and Lara et al. (2018) showed how fine-
671 scale variations underpin larger-scale patterns of change in arctic landscapes. Our results show
672 how such fine-scale variability in abiotic site factors and plant communities can drive different
673 biomass growth patterns under climatic warming and increasing CO_2 concentrations within a
674 land surface model.
675 The AS plant community stood out in our simulation results, highlighting the
676 counteracting effects of biotic and abiotic factors in driving model outcomes. The AS community
677 had shallow soils (Table 1), and as a result when soil depth differences but not arctic PFT
678 parameterizations were included (Simulation 2) the model simulated less biomass in AS than in
679 the E3SM grid cell (Simulation 1). However, in observations of alder shrubs the AS community
680 had by a large margin the highest biomass of any Kougarok Hillslope plant community. Only
681 when differences in arctic plant traits were incorporated, including higher wood allocation and
682 lower fine-root allocation of alders as well as the alleviation of N limitation in the alder-
683 dominated community (Simulation 3), was the model able to reproduce the observed pattern.
684 Even with these changes, the model somewhat underestimated total alder biomass in the AS
685 community, suggesting that additional factors might be missing from the current model
686 configuration. Previous measurements at the Kougarok site showed that alders living in the AS
687 community have trait differences from alders in the ASV community, including taller growth
688 forms, denser shrub-dominated patches, and different rates of N fixation (Salmon et al., 2019a),
689 however model simulations treated them as identical PFTs. Hydrological drainage patterns
690 differed between the AS and ASV communities, with ASV more likely to retain water,
691 potentially stressing alder growth. Leaf stoichiometry also suggested that P availability was
692 higher in the AS community. These hydrological and nutrient factors were not included as cross-
693 community differences in the model configuration for the present study. In addition, N fixation
694 in ELM is empirical rather than process-based, and does not include nodulation, P limitation, or
695 differences in N availability to different PFTs. Improvements to the N fixation model might
696 allow more accurate simulation of the dynamics of N-fixing alder shrubs. For example,
697 associating high N fixation rates directly with alder shrubs and giving that PFT preferential

access to the newly-fixed N could allow an increase in alder shrub productivity without introducing bias in productivity estimates for other plant types co-occurring with alder.

This study focused on plant communities in one intensive study area on the Seward Peninsula of Alaska in the low Arctic in close proximity to latitudinal treeline. As a result, it likely underestimates the full diversity of vegetation traits across the Arctic region. Despite this limitation, the Kougarok Hillslope site adds to our understanding of tundra plant traits, which along with other Arctic environmental measurements are often quantified in only a few locations in the world (Bjorkman et al., 2018; Metcalfe et al., 2018; Virkkala et al., 2019). The PFTs identified in our study matched well with trait-based classifications, particularly size-related traits, identified as covering most of the variability in Arctic plant traits (Thomas et al., 2019), including more accurate ratios of belowground biomass allocation observed in tundra plant communities (Iversen et al., 2015). The plant communities in our study area included multiple shrub-dominated community types (AS, WBT) with low or tall shrubs that are typical of the low Arctic and less common in the high Arctic. Understanding and accurately modeling the traits of shrub-dominated plant communities is important for predicting the future of the Arctic, where shrub expansion is an important ongoing process with significant effects on both biogeochemistry and biophysical land-atmosphere interactions (Bonfils et al., 2012; Euskirchen et al., 2009; Tape et al., 2006; Wilcox et al., 2019). However, a full understanding and accurate prediction of Arctic responses to warming climate will require sampling across a broad range of climates and plant communities (Thomas et al., 2020).

Along with increases in total biomass, our simulations projected changes in relative biomass of different PFTs over the 21st century (Fig. 9). In the TT community, the model predicted an increase in graminoid biomass overcoming shrub PFTs. Graminoids and low deciduous shrubs were also projected to increase relative to other PFTs in the ASV community. These projections reflect differences in biomass accumulation potential, but omit some processes that could be important drivers of future changes. First, the version of ELM used in our simulations does not represent height-structured competition for light among PFTs or the impact of increased leaf litter on lichens and bryophytes. As biomass increases in the future, low-statured vegetation such as dwarf shrubs, lichens and bryophytes could be shaded out by taller shrubs, graminoids and forbs (Elmendorf et al., 2012a; Myers-Smith et al., 2011; M. D. Walker et al., 2006). Our simulations likely overestimate the potential future growth of short-statured vegetation by omitting this effect. Ongoing developments to incorporate height-structured light competition among PFTs in ELM will help to address this issue in the future (Koven et al., 2020). Second, our simulations of historical and future changes in vegetation biomass assumed constant relative areas of different PFTs within each plant community and did not calculate changes in the relative areas of the plant communities due to either climate change or disturbances. As a result, our results may underestimate the potential for future biomass accumulation connected with shrub expansion. For example, the area of the AS plant community on the Kougarok Hillslope has increased over recent decades (Salmon et al., 2019a). The much higher biomass of the AS community compared to other communities at the study site suggests a high potential for biomass accumulation under future shrub expansion. This highlights the need for model simulations of the Arctic region to incorporate either projections of changes in plant community areas or direct simulations of changing species cover using dynamic vegetation and demographic processes (Druel et al., 2019; Fisher et al., 2018).

Other ecosystem and land surface models have been developed for Arctic ecosystems, with varying capabilities and levels of complexity. Arctic-specific models have been designed to

represent plant communities and their variability at a high level of detail. For example, the TEM model (Euskirchen et al., 2009) was designed specifically for improved representation of high-latitude processes. It includes 26 high-latitude PFTs including variations in parameterizations for different ecosystems. Land surface models similar to ELM tend to be limited in the specificity of their PFTs due to the necessity of representing ecosystems across continental to global spatial scales (Wullschleger et al., 2014). However, progress has been made in parameterizing Arctic-specific vegetation types in other models. For example, northern shrubs and mosses were added to the ORCHIDEE land surface model, allowing more realistic simulation of vegetation spatial distributions in boreal regions (Druel et al., 2019). Our results underscore the value of such activities and suggest that better representation of plant diversity in Arctic ecosystems will improve the quality of Earth system model projections of Arctic feedbacks to a changing climate. Rich emerging datasets of Arctic vegetation traits and plant-soil interactions (Bjorkman et al., 2018; Iversen et al., 2015; Thomas et al., 2020) provide opportunities to further improve models such as ELM by targeting key processes including PFT-specific N fixation patterns, root function, vegetation-snow interactions, and plant species demography.

5 Conclusions:

We used intensive field measurements to develop updated model PFTs and parameters representing the diversity of plant functional types observed in the Seward Peninsula of Alaska, USA. New PFTs included forbs, nonvascular plants, and multiple shrub types with different potential heights and leaf habits. Updated PFTs drove differences in contemporary and projected biomass and improved representation of the variability in biomass across different plant communities in the study area, particularly for highly productive alder shrublands. Updated parameterizations also improved simulations of belowground biomass allocation, which was underestimated in the default model. When projected into future climate conditions (RCP 8.5 through 2100), updated arctic PFTs showed increased vegetation C storage, especially in shrub-dominated communities. Our results highlight the importance of representing the diversity of vegetation types and abiotic soil factors in modeling Arctic ecosystems.

6 Acknowledgements

We would like to thank Mary's Igloo Native Corporation for allowing us to perform this research on their land and giving us the opportunity to share this research with their community. Thanks to Shawn Serbin and Alistair Rogers for helpful discussions. Holly Vander Stel, Joanne Childs, and Stan Wullschleger helped with collection of field data and Terri Velliquette was instrumental in data archival. Thanks to Nathan Armistead for graphic design of Figure 2. Contributions to this work from PET and BNS are supported in part by the Energy Exascale Earth System Model (E3SM) project, funded by the U.S. Department of Energy, Office of Science, Office of Biological and Environmental Research. The NGEE Arctic project is supported by the Office of Biological and Environmental Research in the US Department of Energy's Office of Science.

Data availability: Measurements used in model parameterization are archived at the NGEE Arctic Data Repository as cited in the manuscript. Forcing data, model output, and scripts used

for model configuration and data analysis are also archived at the NGEE Arctic Data Repository (Sulman et al., 2020).

7 References

Aerts, R., Bakker, C., & De Caluwe, H. (1992). Root turnover as determinant of the cycling of C, N, and P in a dry heathland ecosystem. *Biogeochemistry*, *15*(3), 175–190.

Beringer, J., Lynch, A. H., Chapin, F. S., Mack, M., & Bonan, G. B. (2001). The Representation of Arctic Soils in the Land Surface Model: The Importance of Mosses. *Journal of Climate*, *14*(15), 3324–3335. https://doi.org/10.1175/1520-0442(2001)014<3324:TROASI>2.0.CO;2

Berner, L. T., Alexander, H. D., Loranty, M. M., Ganzlin, P., Mack, M. C., Davydov, S. P., & Goetz, S. J. (2015). Biomass allometry for alder, dwarf birch, and willow in boreal forest and tundra ecosystems of far northeastern Siberia and north-central Alaska. *Forest Ecology and Management*, *337*, 110–118. https://doi.org/10.1016/j.foreco.2014.10.027

Bhatt, U. S., Walker, D. A., Raynolds, M. K., Bieniek, P. A., Epstein, H. E., Comiso, J. C., et al. (2017). Changing seasonality of panarctic tundra vegetation in relationship to climatic variables. *Environmental Research Letters*, *12*(5). https://doi.org/10.1088/1748-9326/aa6b0b

Bieniek, P., Alaska Climate Adaptation and Science Center, & Lindgren, M. (2020). Historical and Projected Dynamically Downscaled Climate Data for the State of Alaska and surrounding regions at 20km spatial resolution and hourly temporal resolution. Fairbanks, AK: Scenarios Network for Alaska and Arctic Planning, International Arctic Research Center, University of Alaska, Fairbanks. Retrieved from http://ckan.snap.uaf.edu/dataset/historical-and-projected-dynamically-downscaled-climate-data-for-the-state-of-alaska-and-surrou

Bjorkman, A. D., Myers-Smith, I. H., Elmendorf, S. C., Normand, S., Rüger, N., Beck, P. S. A., et al. (2018). Plant functional trait change across a warming tundra biome. *Nature*, *562*(7725), 57–62. https://doi.org/10.1038/s41586-018-0563-7

Bliss, L. C., Heal, O. W., & Moore, J. J. (Eds.). (1981). *Tundra ecosystems: a comparative analysis* (Vol. 25). New York, NY: Cambridge University Press.

Blok, D., Heijmans, M. M. P. D., Schaepman-Strub, G., van Ruijven, J., Parmentier, F. J. W., Maximov, T. C., & Berendse, F. (2011). The Cooling Capacity of Mosses: Controls on Water and Energy Fluxes in a Siberian Tundra Site. *Ecosystems*, *14*(7), 1055–1065. https://doi.org/10.1007/s10021-011-9463-5

Bonfils, C. J. W., Phillips, T. J., Lawrence, D. M., Cameron-Smith, P., Riley, W. J., & Subin, Z. M. (2012). On the influence of shrub height and expansion on northern high latitude climate. *Environmental Research Letters*, *7*(1). https://doi.org/10.1088/1748-9326/7/1/015503

Breen, A., Iversen, C. M., Salmon, V. G., Vander Stel, H., Busey, B., & Wullschleger, S. (2020). NGEE Arctic Plant Traits: Plant Community Composition, Kougarok Road Mile Marker 64, Seward Peninsula, 2016. Oak Ridge, TN: Next Generation Ecosystem Experiments Arctic Data Collection, Oak Ridge National Laboratory. https://doi.org/10.5440/1465967

Bret-Harte, M. S., Shaver, G. R., & Chapin, F. S. (2002). Primary and secondary stem growth in arctic shrubs: Implications for community response to environmental change. *Journal of Ecology*, *90*(2), 251–267. https://doi.org/10.1046/j.1365-2745.2001.00657.x

Bubier, J. L., Smith, R., Juutinen, S., Moore, T. R., Minocha, R., Long, S., & Minocha, S.

(2011). Effects of nutrient addition on leaf chemistry, morphology, and photosynthetic capacity of three bog shrubs. *Oecologia*, *167*(2), 355–368.
Burrows, S. M., Maltrud, M., Yang, X., Zhu, Q., Jeffery, N., Shi, X., et al. (2020). The DOE E3SM v1.1 Biogeochemistry Configuration: Description and Simulated Ecosystem-Climate Responses to Historical Changes in Forcing. *Journal of Advances in Modeling Earth Systems*, *12*(9). https://doi.org/10.1029/2019MS001766
Chapin, F. S., Bret-Harte, M. S., Hobbie, S. E., & Zhong, H. (1996). Plant functional types as predictors of transient responses of arctic vegetation to global change. *Journal of Vegetation Science*, *7*(3), 347–358. https://doi.org/10.2307/3236278
Crittenden, P. D., & Kershaw, K. A. (1978). Discovering the Role of Lichens in the Nitrogen Cycle in Boreal-Arctic Ecosystems. *The Bryologist*, *81*(2), 258. https://doi.org/10.2307/3242187
Druel, A., Ciais, P., Krinner, G., & Peylin, P. (2019). Modeling the Vegetation Dynamics of Northern Shrubs and Mosses in the ORCHIDEE Land Surface Model. *Journal of Advances in Modeling Earth Systems*, *11*(7), 2020–2035. https://doi.org/10.1029/2018MS001531
Elmendorf, S. C., Henry, G. H. R., Hollister, R. D., Björk, R. G., Bjorkman, A. D., Callaghan, T. V., et al. (2012a). Global assessment of experimental climate warming on tundra vegetation: heterogeneity over space and time. *Ecology Letters*, *15*(2), 164–175. https://doi.org/10.1111/j.1461-0248.2011.01716.x
Elmendorf, S. C., Henry, G. H. R., Hollister, R. D., Björk, R. G., Boulanger-Lapointe, N., Cooper, E. J., et al. (2012b). Plot-scale evidence of tundra vegetation change and links to recent summer warming. *Nature Climate Change*, *2*(6), 453–457. https://doi.org/10.1038/nclimate1465
Epstein, H. E., Chapin, F. S., Walker, M. D., & Starfield, A. M. (2001). Analyzing the functional type concept in arctic plants using a dynamic vegetation model. *Oikos*, *95*(2), 239–252. https://doi.org/10.1034/j.1600-0706.2001.950206.x
Epstein, H. E., Raynolds, M. K., Walker, D. A., Bhatt, U. S., Tucker, C. J., & Pinzon, J. E. (2012). Dynamics of aboveground phytomass of the circumpolar Arctic tundra during the past three decades. *Environmental Research Letters*, *7*(1). https://doi.org/10.1088/1748-9326/7/1/015506
Euskirchen, E. S., McGuire, A. D., Chapin, F. S., Yi, S., & Thompson, C. C. (2009). Changes in vegetation in northern Alaska under scenarios of climate change, 2003-2100: implications for climate feedbacks. *Ecological Applications*, *19*(4), 1022–1043. https://doi.org/10.1890/08-0806.1
Fisher, R. A., Koven, C. D., Anderegg, W. R. L., Christoffersen, B. O., Dietze, M. C., Farrior, C. E., et al. (2018). Vegetation demographics in Earth System Models: A review of progress and priorities. *Global Change Biology*, *24*(1), 35–54. https://doi.org/10.1111/gcb.13910
Golaz, J., Caldwell, P. M., Van Roekel, L. P., Petersen, M. R., Tang, Q., Wolfe, J. D., et al. (2019). The DOE E3SM Coupled Model Version 1: Overview and Evaluation at Standard Resolution. *Journal of Advances in Modeling Earth Systems*, *11*(7), 2089–2129. https://doi.org/10.1029/2018MS001603
Gornall, J. L., Jónsdóttir, I. S., Woodin, S. J., & Van der Wal, R. (2007). Arctic mosses govern below-ground environment and ecosystem processes. *Oecologia*, *153*(4), 931–941. https://doi.org/10.1007/s00442-007-0785-0
Van Groenendael, J. M., Kliimeš, L., Klimešová, J., & Hendriks, R. J. J. (1996). Comparative ecology of clonal plants. *Philosophical Transactions of the Royal Society of London. Series*

B: Biological Sciences, *351*(1345), 1331–1339. https://doi.org/10.1098/rstb.1996.0116
Hartmann, D. L., Klein Tank, A. M. G., Rusticucci, M., Alexander, L. V., Brönnimann, S., Chabari, Y., et al. (2013). Observations: Atmosphere and Surface. In T. F. Stocker, D. Qin, G.-K. Plattner, M. Tignor, S. K. Allen, J. Boschung, et al. (Eds.), *Climate Change 2013 - The Physical Science Basis. Contribution of Working Group I to the Fifth Assessment Report of the Intergovernmental Panel on Climate Change* (pp. 159–254). Cambridge: Cambridge University Press.
Hugelius, G., Strauss, J., Zubrzycki, S., Harden, J. W., Schuur, E. A. G., Ping, C. L., et al. (2014). Estimated stocks of circumpolar permafrost carbon with quantified uncertainty ranges and identified data gaps. *Biogeosciences*, *11*(23), 6573–6593. https://doi.org/10.5194/bg-11-6573-2014
Ito, A., Nishina, K., & Noda, H. M. (2016). Impacts of future climate change on the carbon budget of northern high-latitude terrestrial ecosystems: An analysis using ISI-MIP data. *Polar Science*, *10*(3), 346–355. https://doi.org/10.1016/j.polar.2015.11.002
Iversen, C. M., Sloan, V. L., Sullivan, P. F., Euskirchen, E. S., McGuire, A. D., Norby, R. J., et al. (2015). The unseen iceberg: plant roots in arctic tundra. *New Phytologist*, *205*(1), 34–58. https://doi.org/10.1111/nph.13003
Iversen, C. M., Breen, A., Salmon, V. G., Vander Stel, H., & Wullschleger, S. D. (2017). NGEE Arctic Plant Traits: Vegetation Plot Locations, Ecotypes, and Photos, Kougarok Road Mile Marker 64, Seward Peninsula, Alaska, 2016. Oak Ridge, TN: Next Generation Ecosystem Experiments Arctic Data Collection, Oak Ridge National Laboratory. https://doi.org/10.5440/1346196
Iversen, C. M., Breen, A., Salmon, V. G., Vander Stel, H., & Wullschleger, S. (2019a). NGEE Arctic Plant Traits: Soil Depth, Kougarok Road Mile Marker 64, Seward Peninsula, Alaska, beginning 2016. Oak Ridge, TN: Next Generation Ecosystem Experiments Arctic Data Collection, Oak Ridge National Laboratory. https://doi.org/10.5440/1346198
Iversen, C. M., Salmon, V. G., Breen, A., Vander Stel, H., & Wullschleger, S. (2019b). NGEE Arctic Plant Traits: Soil Temperature and Moisture, Kougarok Road Mile Marker 64, Seward Peninsula, Alaska, beginning 2016. Oak Ridge, TN: Next Generation Ecosystem Experiments Arctic Data Collection, Oak Ridge National Laboratory. https://doi.org/10.5440/1346195
Jackson, R. B., Lajtha, K., Crow, S. E., Hugelius, G., Kramer, M. G., & Piñeiro, G. (2017). The Ecology of Soil Carbon: Pools, Vulnerabilities, and Biotic and Abiotic Controls. *Annual Review of Ecology, Evolution, and Systematics*, *48*(1), 419–445. https://doi.org/10.1146/annurev-ecolsys-112414-054234
Jia, G. J., Epstein, H. E., & Walker, D. A. (2003). Greening of arctic Alaska, 1981-2001. *Geophysical Research Letters*, *30*(20), 3–6. https://doi.org/10.1029/2003GL018268
Joly, K., Jandt, R. R., & Klein, D. R. (2009). Decrease of lichens in Arctic ecosystems: The role of wildfire, caribou, reindeer, competition and climate in north-western Alaska. *Polar Research*, *28*(3), 433–442. https://doi.org/10.1111/j.1751-8369.2009.00113.x
Jonasson, S., & Chapin, F. S. (1985). Significance of sequential leaf development for nutrient balance of the cotton sedge, Eriophorum vaginatum L. *Oecologia*, *67*(4), 511–518. https://doi.org/10.1007/BF00790022
Kellner, E. (2001). Surface energy fluxes and control of evapotranspiration from a Swedish Sphagnum mire. *Agricultural and Forest Meteorology*, *110*(2), 101–123.
Klimešová, J., Martínková, J., & Herben, T. (2018). Horizontal growth: An overlooked

dimension in plant trait space. *Perspectives in Plant Ecology, Evolution and Systematics*, *32*(February), 18–21. https://doi.org/10.1016/j.ppees.2018.02.002

Koven, C. D., Ringeval, B., Friedlingstein, P., Ciais, P., Cadule, P., Khvorostyanov, D., et al. (2011). Permafrost carbon-climate feedbacks accelerate global warming. *Proceedings of the National Academy of Sciences*, *108*(36), 14769–14774. https://doi.org/10.1073/pnas.1103910108

Koven, C. D., Riley, W. J., Subin, Z. M., Tang, J. Y., Torn, M. S., Collins, W. D., et al. (2013). The effect of vertically resolved soil biogeochemistry and alternate soil C and N models on C dynamics of CLM4. *Biogeosciences*, *10*(11), 7109–7131. https://doi.org/10.5194/bg-10-7109-2013

Koven, C. D., Knox, R. G., Fisher, R. A., Fisher, R. A., Chambers, J. Q., Chambers, J. Q., et al. (2020). Benchmarking and parameter sensitivity of physiological and vegetation dynamics using the Functionally Assembled Terrestrial Ecosystem Simulator (FATES) at Barro Colorado Island, Panama. *Biogeosciences*, *17*(11), 3017–3044. https://doi.org/10.5194/bg-17-3017-2020

Lange, O. L., Hahn, S. C., Meyer, A., & Tenhunen, J. D. (1998). Upland Tundra in the Foothills of the Brooks Range, Alaska, U.S.A.: Lichen Long-Term Photosynthetic CO 2 Uptake and Net Carbon Gain. *Arctic and Alpine Research*, *30*(3), 252. https://doi.org/10.2307/1551972

Lara, M. J., Nitze, I., Grosse, G., Martin, P., & David McGuire, A. (2018). Reduced arctic tundra productivity linked with landform and climate change interactions. *Scientific Reports*, *8*(1), 1–10. https://doi.org/10.1038/s41598-018-20692-8

Lawrence, D. M., Fisher, R. A., Koven, C. D., Oleson, K. W., Swenson, S. C., Bonan, G., et al. (2019). The Community Land Model Version 5: Description of New Features, Benchmarking, and Impact of Forcing Uncertainty. *Journal of Advances in Modeling Earth Systems*, *11*(12), 4245–4287. https://doi.org/10.1029/2018MS001583

Longton, R. E. (1997). The role of bryophytes and lichens in polar ecosystems. In M. Marquiss & S. J. Woodin (Eds.), *Ecology of Arctic Environments: 13th Special Symposium of the British Ecological Society* (pp. 69–96). Cambridge University Press.

Loranty, M. M., Berner, L. T., Goetz, S. J., Jin, Y., & Randerson, J. T. (2014). Vegetation controls on northern high latitude snow-albedo feedback: Observations and CMIP5 model simulations. *Global Change Biology*, *20*(2), 594–606. https://doi.org/10.1111/gcb.12391

Loranty, M. M., Abbott, B. W., Blok, D., Douglas, T. A., Epstein, H. E., Forbes, B. C., et al. (2018). Reviews and syntheses: Changing ecosystem influences on soil thermal regimes in northern high-latitude permafrost regions. *Biogeosciences*, *15*(17), 5287–5313. https://doi.org/10.5194/bg-15-5287-2018

McGuire, A. D., Christensen, T. R., Hayes, D., Heroult, A., Euskirchen, E., Kimball, J. S., et al. (2012). An assessment of the carbon balance of Arctic tundra: comparisons among observations, process models, and atmospheric inversions. *Biogeosciences*, *9*(8), 3185–3204. Retrieved from http://www.biogeosciences.net/9/3185/2012/

Metcalfe, D. B., Hermans, T. D. G., Ahlstrand, J., Becker, M., Berggren, M., Björk, R. G., et al. (2018). Patchy field sampling biases understanding of climate change impacts across the Arctic. *Nature Ecology and Evolution*, *2*(9), 1443–1448. https://doi.org/10.1038/s41559-018-0612-5

Monson, R. K., Lipson, D. L., Burns, S. P., Turnipseed, A. A., Delany, A. C., Williams, M. W., & Schmidt, S. K. (2006). Winter forest soil respiration controlled by climate and microbial community composition. *Nature*, *439*(7077), 711–714. https://doi.org/10.1038/nature04555

Myers-Smith, I. H., & Hik, D. S. (2013). Shrub canopies influence soil temperatures but not nutrient dynamics: An experimental test of tundra snow-shrub interactions. *Ecology and Evolution*, *3*(11), 3683–3700. https://doi.org/10.1002/ece3.710

Myers-Smith, I. H., Forbes, B. C., Wilmking, M., Hallinger, M., Lantz, T., Blok, D., et al. (2011). Shrub expansion in tundra ecosystems: Dynamics, impacts and research priorities. *Environmental Research Letters*, *6*(4). https://doi.org/10.1088/1748-9326/6/4/045509

Myers-Smith, I. H., Elmendorf, S. C., Beck, P. S. A., Wilmking, M., Hallinger, M., Blok, D., et al. (2015). Climate sensitivity of shrub growth across the tundra biome. *Nature Climate Change*, *5*(9), 887–891. https://doi.org/10.1038/nclimate2697

Myers-Smith, I. H., Grabowski, M. M., Thomas, H. J. D., Angers-Blondin, S., Daskalova, G. N., Bjorkman, A. D., et al. (2019). Eighteen years of ecological monitoring reveals multiple lines of evidence for tundra vegetation change. *Ecological Monographs*, *0*(0), e01351. https://doi.org/10.1002/ecm.1351

Myers-Smith, I. H., Kerby, J. T., Phoenix, G. K., Bjerke, J. W., Epstein, H. E., Assmann, J. J., et al. (2020). Complexity revealed in the greening of the Arctic. *Nature Climate Change 2020 10:2*, *10*(2), 106–117. https://doi.org/10.1038/s41558-019-0688-1

Nash, T. H., Moser, T. J., Link, S. O., Ross, L. J., Olafsen, A., & Matthes, U. (1983). Lichen photosynthesis in relation to CO 2 concentration. *Oecologia*, *58*(1), 52–56.

Oleson, K. W., Lawrence, D. M., Bonan, G. B., Drewniak, B., Huang, M., Charles, D., et al. (2013). Technical description of version 4.5 of the Community Land Model (CLM), (July). https://doi.org/10.5065/D6RR1W7M

Pearson, R. G., Phillips, S. J., Loranty, M. M., Beck, P. S. A., Damoulas, T., Knight, S. J., & Goetz, S. J. (2013). Shifts in Arctic vegetation and associated feedbacks under climate change. *Nature Climate Change*, *3*(7), 673–677. https://doi.org/10.1038/nclimate1858

Porada, P., Ekici, A., & Beer, C. (2016). Effects of bryophyte and lichen cover on permafrost soil temperature at large scale. *Cryosphere*, *10*(5), 2291–2315. https://doi.org/10.5194/tc-10-2291-2016

Qian, H., Joseph, R., & Zeng, N. (2010). Enhanced terrestrial carbon uptake in the northern high latitudes in the 21st century from the Coupled Carbon Cycle Climate Model Intercomparison Project model projections. *Global Change Biology*, *16*(2), 641–656. https://doi.org/10.1111/j.1365-2486.2009.01989.x

Rasse, D. P., Rumpel, C., & Dignac, M. F. (2005). Is soil carbon mostly root carbon? Mechanisms for a specific stabilisation. *Plant and Soil*, *269*, 341–356. Retrieved from http://www.springerlink.com/index/L543334M54177X4T.pdf

Raynolds, M. K., Walker, D. A., Balser, A., Bay, C., Campbell, M., Cherosov, M. M., et al. (2019). A raster version of the Circumpolar Arctic Vegetation Map (CAVM). *Remote Sensing of Environment*, *232*(July). https://doi.org/10.1016/j.rse.2019.111297

Ricciuto, D., Sargsyan, K., & Thornton, P. (2018). The Impact of Parametric Uncertainties on Biogeochemistry in the E3SM Land Model. *Journal of Advances in Modeling Earth Systems*, *10*(2), 297–319. https://doi.org/10.1002/2017MS000962

Rogers, A. (2014). The use and misuse of Vc,max in Earth System Models. *Photosynthesis Research*, *119*(1–2), 15–29. https://doi.org/10.1007/s11120-013-9818-1

Rogers, A., Serbin, S. P., Ely, K. S., Sloan, V. L., & Wullschleger, S. D. (2017). Terrestrial biosphere models underestimate photosynthetic capacity and CO 2 assimilation in the Arctic. *New Phytologist*, *216*(4), 1090–1103. https://doi.org/10.1111/nph.14740

Ruess, R. W., Van Cleve, K., Yarie, J., & Viereck, L. A. (1996). Contributions of fine root

production and turnover to the carbon and nitrogen cycling in taiga forests of the Alaskan interior. *Canadian Journal of Forest Research*, *26*(8), 1326–1336. https://doi.org/10.1139/x26-148

Salmon, V. G., Soucy, P., Mauritz, M., Celis, G., Natali, S. M., Mack, M. C., & Schuur, E. A. G. (2016). Nitrogen availability increases in a tundra ecosystem during five years of experimental permafrost thaw. *Global Change Biology*, *22*(5), 1927–1941. https://doi.org/10.1111/gcb.13204

Salmon, V. G., Breen, A. L., Kumar, J., Lara, M. J., Thornton, P. E., Wullschleger, S. D., & Iversen, C. M. (2019a). Alder Distribution and Expansion Across a Tundra Hillslope: Implications for Local N Cycling. *Frontiers in Plant Science*, *10*, 1099. https://doi.org/10.3389/fpls.2019.01099

Salmon, V. G., Iversen, C. M., Breen, A., Vander Stel, H., & Childs, J. (2019b). NGEE Arctic Plant Traits: Plant Biomass and Traits, Kougarok Road Mile Marker 64, Seward Peninsula, Alaska, beginning 2016. Oak Ridge, TN: Next Generation Ecosystem Experiments Arctic Data Collection, Oak Ridge National Laboratory. https://doi.org/10.5440/1346199

Salmon, V. G., Iversen, C. M., Childs, J., & Vander Stel, H. (2019c). NGEE Arctic Plant Traits: Soil Cores, Kougarok Road Mile Marker 64, Seward Peninsula, Alaska, 2016. Oak Ridge, TN: Next Generation Ecosystem Experiments Arctic Data Collection, Oak Ridge National Laboratory. https://doi.org/10.5440/1346200

Salmon, V. G., Iversen, C. M., Breen, A., Childs, J., Vander Stel, H., & Wullschleger, S. (2019d). NGEE Arctic Plant Traits: Soil Nutrient Availability, Seward Peninsula, Alaska, beginning 2016. Oak Ridge, TN: Next Generation Ecosystem Experiments Arctic Data Collection, Oak Ridge National Laboratory. https://doi.org/10.5440/1346201

Schuur, E. A. G., McGuire, A. D., Schädel, C., Grosse, G., Harden, J. W., Hayes, D. J., et al. (2015). Climate change and the permafrost carbon feedback. *Nature*, *520*(7546), 171–179. https://doi.org/10.1038/nature14338

Shaver, G. R., & Billings, W. D. (1975). Root Production and Root Turnover in a Wet Tundra Ecosystem, Barrow, Alaska. *Ecology*, *56*(2), 401–409. https://doi.org/10.2307/1934970

Shaver, G. R., & Chapin, F. S. (1991). Production: Biomass Relationships and Element Cycling in Contrasting Arctic Vegetation Types. *Ecological Monographs*, *61*(1), 1–31. https://doi.org/10.2307/1942997

Shaver, G. R., & Laundre, J. (1997). Exsertion, elongation, and senescence of leaves of Eriophorum vaginatum and Carex bigelowii in Northern Alaska. *Global Change Biology*, *3*(S1), 146–157. https://doi.org/10.1111/j.1365-2486.1997.gcb141.x

Shaver, G. R., Billings, W. D., Chapin, F. S., Giblin, A. E., Nadelhoffer, K. J., Oechel, W. C., & Rastetter, E. B. (1992). Global Change and the Carbon Balance of Arctic Ecosystems. *BioScience*, *42*(6), 433–441. https://doi.org/10.2307/1311862

Shi, X., Ricciuto, D. M., Thornton, P. E., Xu, X., Yuan, F., Meng, L., et al. (2020). Modeling the hydrology and physiology of Sphagnum moss in a northern temperate bog. *Biogeosciences Discussions*, (May), in review. Retrieved from https://doi.org/10.5194/bg-2020-90

Song, X., Hoffman, F. M., Iversen, C. M., Yin, Y., Kumar, J., Ma, C., & Xu, X. (2017). Significant inconsistency of vegetation carbon density in CMIP5 Earth system models against observational data. *Journal of Geophysical Research: Biogeosciences*, *122*(9), 2282–2297. https://doi.org/10.1002/2017JG003914

Stoy, P., Street, L., Johnson, A., Prieto-Blanco, A., & Ewing, S. (2012). Temperature, heat flux, and reflectance of common subarctic mosses and lichens under field conditions: Might

changes to community composition impact climate-relevant surface fluxes? *Arctic, Antarctic, and Alpine Research*, *44*(4), 500–508. https://doi.org/10.1657/1938-4246-44.4.500

Sturm, M., Holmgren, J., McFadden, J. P., Liston, G. E., Chapin, F. S., & Racine, C. H. (2001). Snow–Shrub Interactions in Arctic Tundra: A Hypothesis with Climatic Implications. *Journal of Climate*, *14*(3), 336–344. https://doi.org/10.1175/1520-0442(2001)014<0336:SSIIAT>2.0.CO;2

Sturm, M., Douglas, T., Racine, C., & Liston, G. E. (2005). Changing snow and shrub conditions affect albedo with global implications. *Journal of Geophysical Research*, *110*(G1), G01004. https://doi.org/10.1029/2005JG000013

Sullivan, P. F., Sommerkorn, M., Rueth, H. M., Nadelhoffer, K. J., Shaver, G. R., & Welker, J. M. (2007). Climate and species affect fine root production with long-term fertilization in acidic tussock tundra near Toolik Lake, Alaska. *Oecologia*, *153*(3), 643–652. https://doi.org/10.1007/s00442-007-0753-8

Sulman, B. N., Salmon, V. G., Iversen, C. M., Breen, A. L., Yuan, F., & Thornton, P. E. (2020). Integrating New Arctic Plant Functional Types in a Land Surface Model Using Above- and Belowground Field Observations: Modeling Archive. Oak Ridge, TN: Next Generation Ecosystem Experiments Arctic Data Collection, Oak Ridge National Laboratory. Retrieved from https://ngee-arctic.ornl.gov/data/pages/NGA234.html

Tape, K., Sturm, M., & Racine, C. (2006). The evidence for shrub expansion in Northern Alaska and the Pan-Arctic. *Global Change Biology*, *12*(4), 686–702. https://doi.org/10.1111/j.1365-2486.2006.01128.x

Thomas, H. J. D., Myers-Smith, I. H., Bjorkman, A. D., Elmendorf, S. C., Blok, D., Cornelissen, J. H. C., et al. (2019). Traditional plant functional groups explain variation in economic but not size-related traits across the tundra biome. *Global Ecology and Biogeography*, *28*(2), 78–95. https://doi.org/10.1111/geb.12783

Thomas, H. J. D., Bjorkman, A. D., Myers-Smith, I. H., Elmendorf, S. C., Kattge, J., Diaz, S., et al. (2020). Global plant trait relationships extend to the climatic extremes of the tundra biome. *Nature Communications 2020 11:1*, *11*(1), 1–12. https://doi.org/10.1038/s41467-020-15014-4

Thornton, P. E., & Rosenbloom, N. A. (2005). Ecosystem model spin-up: Estimating steady state conditions in a coupled terrestrial carbon and nitrogen cycle model. *Ecological Modelling*, *189*(1–2), 25–48. https://doi.org/10.1016/j.ecolmodel.2005.04.008

Turetsky, M. R., Bond-Lamberty, B., Euskirchen, E., Talbot, J., Frolking, S., McGuire, A. D., & Tuittila, E. S. (2012). The resilience and functional role of moss in boreal and arctic ecosystems. *New Phytologist*, *196*(1), 49–67. https://doi.org/10.1111/j.1469-8137.2012.04254.x

Turetsky, M. R., Abbott, B. W., Jones, M. C., Anthony, K. W., Olefeldt, D., Schuur, E. A. G., et al. (2020). Carbon release through abrupt permafrost thaw. *Nature Geoscience*, *13*(2), 138–143. https://doi.org/10.1038/s41561-019-0526-0

Verheijen, L. M., Aerts, R., Brovkin, V., Cavender-Bares, J., Cornelissen, J. H. C., Kattge, J., & van Bodegom, P. M. (2015). Inclusion of ecologically based trait variation in plant functional types reduces the projected land carbon sink in an earth system model. *Global Change Biology*, *21*(8), 3074–3086. https://doi.org/10.1111/gcb.12871

Virkkala, A. M., Abdi, A. M., Luoto, M., & Metcalfe, D. B. (2019). Identifying multidisciplinary research gaps across Arctic terrestrial gradients. *Environmental Research Letters*, *14*(12).

https://doi.org/10.1088/1748-9326/ab4291
Walker, D. A. (1987). Height and growth rings of Salix lanata ssp. richardsonii along the coastal temperature gradient of northern Alaska. *Canadian Journal of Botany*, *65*(5), 988–993. https://doi.org/10.1139/b87-136
Walker, D. A., Reynolds, M. K., Daniëls, F. J. A., Einarsson, E., Elvebakk, A., Gould, W. A., et al. (2005). The Circumpolar Arctic vegetation map. *Journal of Vegetation Science*, *16*(3), 267–282. https://doi.org/10.1111/j.1654-1103.2005.tb02365.x
Walker, D. A., Daniëls, F. J. A., Alsos, I., Bhatt, U. S., Breen, A. L., Buchhorn, M., et al. (2016). Circumpolar Arctic vegetation: A hierarchic review and roadmap toward an internationally consistent approach to survey, archive and classify tundra plot data. *Environmental Research Letters*, *11*(5). https://doi.org/10.1088/1748-9326/11/5/055005
Walker, M. D., Wahren, C. H., Hollister, R. D., Henry, G. H. R., Ahlquist, L. E., Alatalo, J. M., et al. (2006). Plant community responses to experimental warming across the tundra biome. *Proceedings of the National Academy of Sciences of the United States of America*, *103*(5), 1342–1346. https://doi.org/10.1073/pnas.0503198103
Walsh, J. E., Bhatt, U. S., Littell, J. S., Leonawicz, M., Lindgren, M., Kurkowski, T. A., et al. (2018). Downscaling of climate model output for Alaskan stakeholders. *Environmental Modelling and Software*, *110*, 38–51. https://doi.org/10.1016/j.envsoft.2018.03.021
Wielgolaski, F. E. (1972). Vegetation Types and Plant Biomass in Tundra. *Arctic and Alpine Research*, *4*(4), 291–305. https://doi.org/10.1080/00040851.1972.12003650
Wilcox, E. J., Keim, D., de Jong, T., Walker, B., Sonnentag, O., Sniderhan, A. E., et al. (2019). Tundra shrub expansion may amplify permafrost thaw by advancing snowmelt timing. *Arctic Science*, *5*(4), 202–217. https://doi.org/10.1139/as-2018-0028
Williams, T. G., & Flanagan, L. B. (1998). Measuring and modelling environmental influences on photosynthetic gas exchange in Sphagnum and Pleurozium. *Plant, Cell & Environment*, *21*(6), 555–564.
Wullschleger, S. D., Epstein, H. E., Box, E. O., Euskirchen, E. S., Goswami, S., Iversen, C. M., et al. (2014). Plant functional types in Earth system models: Past experiences and future directions for application of dynamic vegetation models in high-latitude ecosystems. *Annals of Botany*, *114*(1), 1–16. https://doi.org/10.1093/aob/mcu077
Yang, X., Ricciuto, D. M., Thornton, P. E., Shi, X., Xu, M., Hoffman, F., & Norby, R. J. (2019). The Effects of Phosphorus Cycle Dynamics on Carbon Sources and Sinks in the Amazon Region: A Modeling Study Using ELM v1. *Journal of Geophysical Research: Biogeosciences*, *124*(12), 3686–3698. https://doi.org/10.1029/2019JG005082
Zeng, X. (2001). Global Vegetation Root Distribution for Land Modeling. *Journal of Hydrometeorology*, *2*(5), 525–530. https://doi.org/10.1175/1525-7541(2001)002<0525:gvrdfl>2.0.co;2

8 Supplementary figures and tables

Figure S1. Comparison between raw data in Berner et al 2015 (grey) and NGEE Arctic destructive harvests of tall shrub species (red).

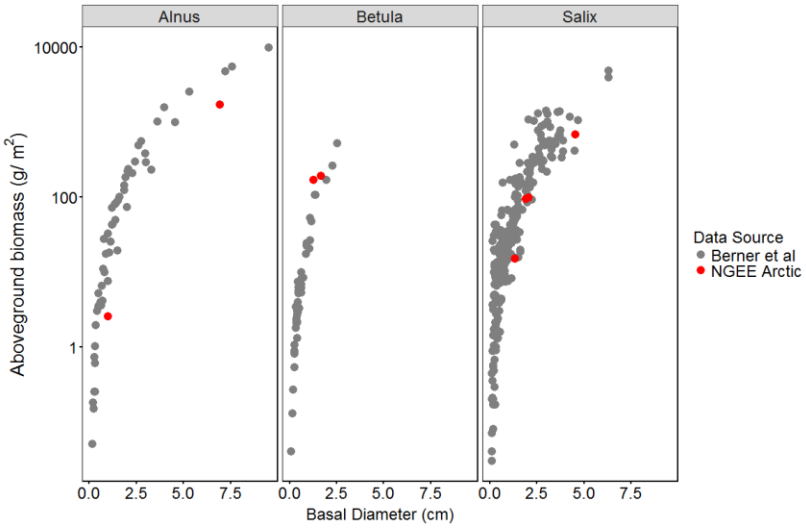

Table S1. Ratio of rhizome biomass to aboveground biomass in Shaver & Chapin 1991

	Rhizome Biomass :Aboveground Biomass		
PFT	Tussock Tundra Community	Shrub Community	Heath Community
Graminoid	0.91	0.36	1.40
Deciduous	1.51	1.07	1.36
Evergreen	1.41	0.17	0.88
Forb	0.89	0.51	NA
All vascular	1.29	1.05	0.99

Table S2. Fine root turnovers in arctic literature

Community	Fine root turnover (years)	Notes
AS	1.33	Sequential soil cores collected in interior AK Alder-Balsam poplar stand (Ruess et al., 1996)
BEL	1.56	From sequential cores in a dry heathland in the Netherlands (evergreen dwarf species) (Aerts et al., 1992)
DLST	1.56	From sequential cores in a dry heathland in the Netherlands (evergreen dwarf species) (Aerts et al., 1992)
TT	3.13	From fine root biomass pools and minirhizotrons in tussock tundra at Toolik (Sullivan et al., 2007). (Shaver & Billings, 1975) estimates from Barrow have turnover time of 4 years but for wet sedge tundra. Tundra at our site is more similar to Toolik plant community so Sullivan's is more applicable
ASV	2.23	Average of Ruess et al. (1996) Alder-Balsam popular and Sullivan et al. (2007) tussock tundra

		number
WBT	1.33	Ruess et al. (1996), sequential soil cores collected in interior AK Alder-Balsam poplar stand

Table S3. Turnover of stems, calculated from aboveground stems and applied to rhizomes

Community	PFT	Stem turnover (years)
AS	Evergreen dwarf shrub	26.55
AS	Deciduous low shrub	25.72
AS	Alder shrub	100.02
AS	Low to tall deciduous birch	29.78
ASV	Evergreen dwarf shrub	13.96
ASV	Deciduous low shrub	22.14
ASV	Alder shrub	80.30
ASV	Low to tall deciduous willow	42.47
WBT	Evergreen dwarf shrub	9.58
WBT	Deciduous low shrub	22.97
WBT	Low to tall deciduous birch	21.73
WBT	Low to tall deciduous willow	92.11
BEL	Dwarf evergreen shrub	24.63
BEL	Low deciduous shrub	21.62
TT	Dwarf evergreen shrub	13.18
TT	Low deciduous shrub	13.81
TT	Low to tall deciduous willow	33.6
DLST	Dwarf evergreen shrub	6.25